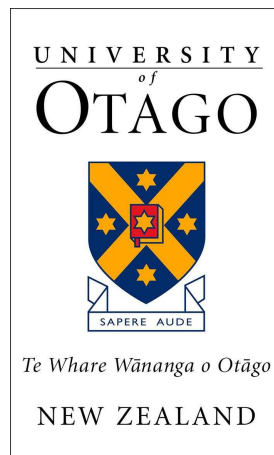


# Self induced temperature gradients in Brownian dynamics

Jack Devine

THE UNIVERSITY OF OTAGO



A THESIS SUBMITTED FOR THE PARTIAL FULFILLMENT  
OF BScHONS IN PHYSICS AT THE UNIVERSITY OF  
OTAGO, DUNEDIN, NEW ZEALAND

supervised by  
Dr M. W. JACK

September 19, 2016

## Abstract

At the atomic level, we have new kinds of forces and new kinds of possibilities, new kinds of effects. The problems of manufacture and reproduction of materials will be quite different. I am, as I said, inspired by the biological phenomena in which chemical forces are used in a repetitious fashion to produce all kinds of weird effects (one of which is the author).

**Richard Feynman**  
– **There's Plenty of room at the bottom (1959).**



# Contents

<b>1</b>	<b>Introduction</b>	<b>1</b>
1.1	Brownian motion . . . . .	1
1.2	Brownian motors . . . . .	4
1.3	Classes of Brownian motors . . . . .	4
1.3.1	Feynman ratchet and pawl . . . . .	5
1.3.2	Landauer's blowtorch . . . . .	6
1.3.3	Tilted periodic potentials . . . . .	7
1.4	Student contributions . . . . .	7
<b>2</b>	<b>Setting up the system</b>	<b>9</b>
2.1	The Smoluchowski equation . . . . .	9
2.2	System thermodynamics . . . . .	11
2.3	Making the equations dimensionless . . . . .	13
<b>3</b>	<b>Solving the system</b>	<b>17</b>
3.1	Steady state solution . . . . .	17
3.2	Finite differences . . . . .	19
3.2.1	Boundary conditions . . . . .	21
3.3	Testing the numerics . . . . .	24
3.3.1	A comparison with analytical results . . . . .	24
3.3.2	Convergence tests . . . . .	25
<b>4</b>	<b>Exploration</b>	<b>29</b>
4.1	Bistable potentials . . . . .	29
4.1.1	Kramer's rate . . . . .	30
4.1.2	The reverse Landauer blowtorch . . . . .	34
4.2	Tilted periodic potentials . . . . .	35
<b>5</b>	<b>Discussion</b>	<b>37</b>
<b>6</b>	<b>Outlook</b>	<b>39</b>
6.1	Generalization to 2d and 3d systems . . . . .	39
6.2	Inter-particle interactions . . . . .	39
6.3	Fluid dynamics . . . . .	40
	<b>Bibliography</b>	<b>41</b>

Appendices	45
A Additional figures	49

# Chapter 1

## Introduction

To mention all the mineral substances in which I have found these molecules, would be tedious; and I shall confine myself in this summary to an enumeration of a few of the most remarkable. These were both of aqueous and igneous origin, as travertine, stalactites, lava, obsidian, pumice, volcanic ashes, and meteorites from various localities. Of metals I may mention manganese, nickel, plumbago, bismuth, antimony, and arsenic. In a word, in every mineral which I could reduce to a powder, sufficiently fine to be temporarily suspended in water, I found these molecules more or less copiously; and in some cases, more particularly in siliceous crystals, the whole body submitted to examination appeared to be composed of them.

---

**Robert Brown, on what we now call Brownian particles**

### 1.1 Brownian motion

Brownian motion is the motion that occurs when looking at microscopic particles that are suspended in a fluid, this motion is highly random and is due to molecules in the fluid colliding with the particle trillions of times per second. Brownian motion occurs on the micro-meter to nano-meter scale [1, 2], particles of this size are constantly bombarded by the environment causing some people to use the term molecular hurricane [3], amazingly though, some systems in biology and in the laboratory are able to create directed motion and draw energy from this chaotic environment [2]. In principle if one knew the momenta and positions of all particles in a system, then one could use Newtonian mechanics to fully predict the future state of the system. However, for systems of interest in this project, we will be looking at systems with particle number on the order of Avagadro's number ( $N \sim 10^{23}$ ). With systems of this size, a Newtonian description is completely impractical, so instead we will use a statistical approach, in this view the motion of a single Brownian particle suspended in a fluid at a given temperature (which we will call the bath) is random, we explain this random motion in Figure 1.1.

Brownian motion was first observed by Robert Brown in 1827 [5], in these observations, Brown saw that microscopic particles (for example pollen grains) were in constant motion. He noticed that this motion was still present in inorganic material including granite and ground up Sphinx bones. Over half a century later,

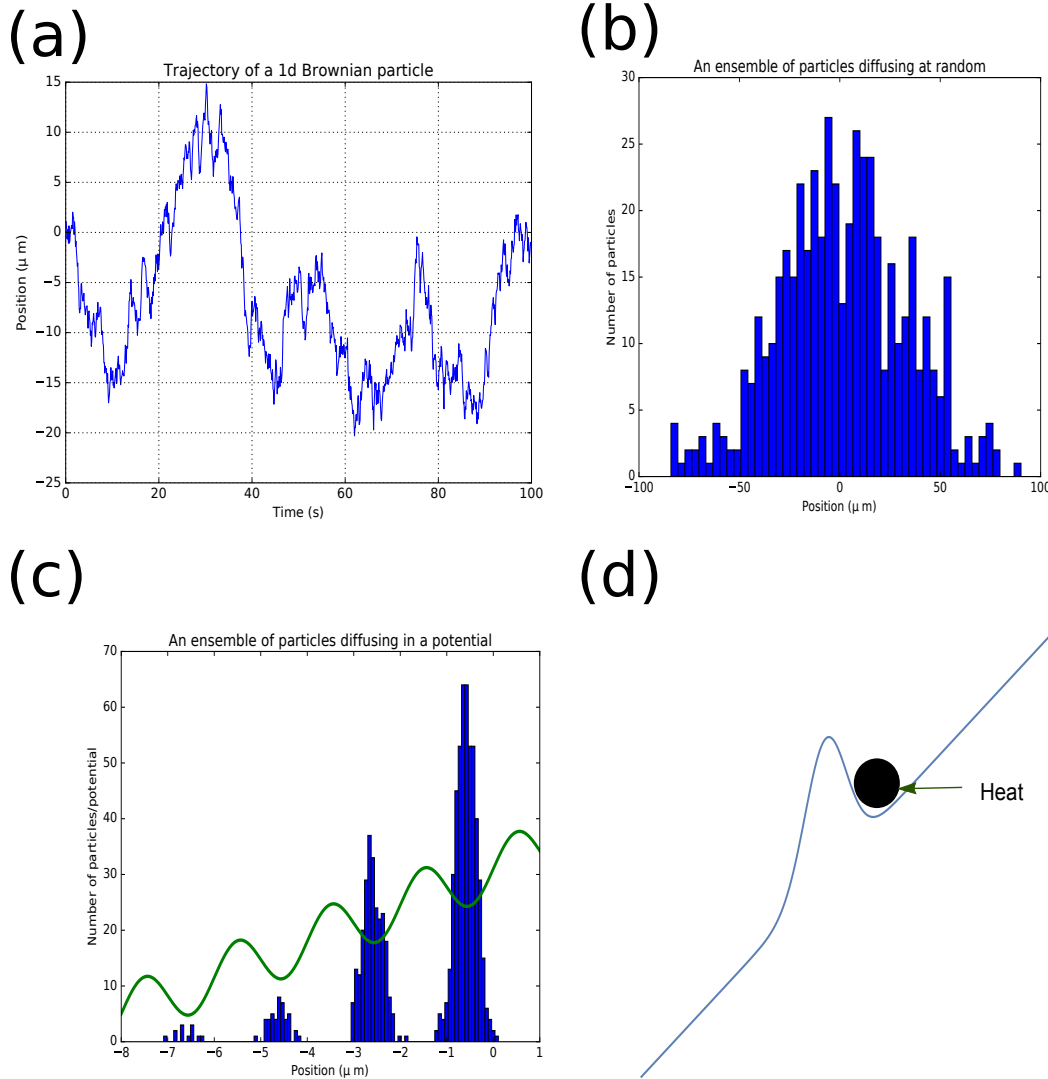


**Figure 1.1: Cartoon demonstration of Brownian motion.** (a) Trajectory of a single tagged Brownian particle, the particle is being forced around randomly by the molecular hurricane, since there is no net force on the particle, we find that the particle makes no net progress over time. (b) An ensemble of Brownian particles simulated for 100 seconds, here we see that the mean movement is zero because there is no background force on the particles, this statistical nature of the particles motivates us to view the particles in a probabilistic sense. (c) The particles can be placed in a potential (for example charged particles in an electric field), initially the particles were all located at  $x = 0$ , after some time we find that the particles have moved to a lower potential energy state and that they tend to situate at the bottom of the wells in the potential. These locations can be approximated by parabolas, it can be shown that in this case, the particles will decay into a Gaussian distribution [4] as we can see in the figure. (d) Zoomed in cartoon of a particle about to jump over a barrier, in Newtonian mechanics the particle would need enough potential energy to simply roll over the barrier, however in this project we will be in the over-damped regime where the particles have no inertia, in order for the particle to get over the barrier there will need to be an event that occurs where many particles will hit the particle on its right hand side. This will cause the bath to lose some energy as heat as shown in the figure, this heat will be the source of the thermal interactions that we will talk about in § 2.1



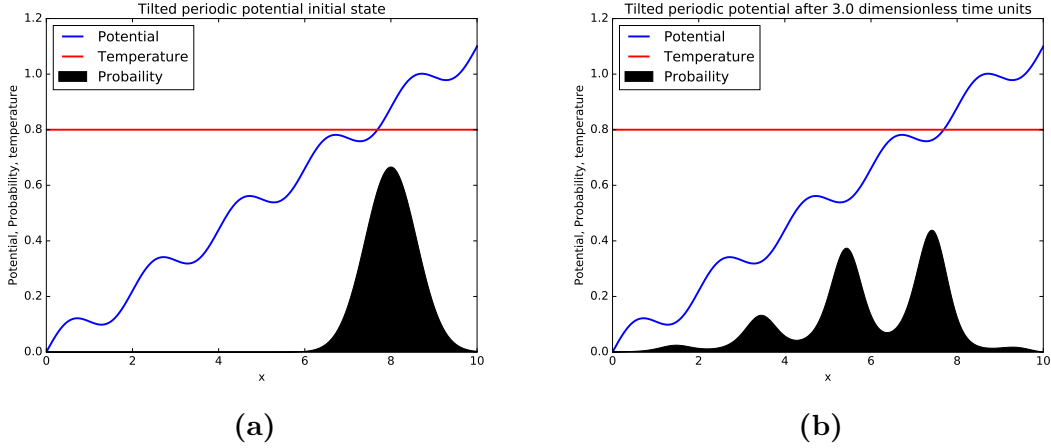


**Figure 1.2:** Schematic showing the probability density of particles diffusing in a one dimensional tilted periodic potential at a fixed temperature. We see that the particles tend to drift down the potential as they diffuse, this drift will be called the current  $J$  which we will quantify in section § 2.1. In section 2.3, we will define the dimensionless time scale and length scale used in the calculations for this figure.

Einstein showed that Brownian motion was due to constant bombardment by water molecules in the surrounding environment [6], Einstein’s theory of Brownian motion was then experimentally verified by Perrin [7].

The regime of Brownian motion that we will discuss is the so called over-damped limit, in this regime particles do not have inertia, so all of the energy of the system is quantified by the potential energy of the particle and the thermal energy of the bath [8–11]. The over-damped regime of a Brownian particle can be described stochastically by the Langevin equation

$$\gamma \dot{x}(t) = -V'(x(t)) + \xi(t) \quad (1.1)$$

Where  $\gamma$  is the viscous friction coefficient of the Brownian particle,  $V(x)$  is the potential that the particle is in and  $\xi(t)$  is Gaussian white noise with zero mean and has auto-correlation given by  $\langle \xi(t)\xi(s) \rangle = 2\gamma k_B T \delta(t-s)$ . This is essentially the stochastic view of Brownian motion, as mentioned earlier we can also describe Brownian motion by following the evolution of the probability distribution of a single Brownian particle.

The probabilistic view of Brownian motion is shown in figure 1.2, here we see the same physical situation as depicted in part (c) of Figure 1.1. The key difference is that in Figure 1.2 we do not have any knowledge of the individual particles in the ensemble, but instead we only know about the probability distribution that describes them. The situation in Figure 1.2 is described by the Smoluchowski equation [12], from now on we will use the Smoluchowski equation to model a Brownian particle, however it is useful to keep in mind that the underlying dynamics are stochastic. The Smoluchowski equation can be written as:

$$\frac{\partial P(x, t)}{\partial t} = \gamma^{-1} \frac{\partial}{\partial x} \left( P(x, t) \frac{\partial V}{\partial x} + k_B T(x, t) \frac{\partial P(x, t)}{\partial x} \right) \quad (1.2)$$

Where  $P(x, t)$  is the probability distribution for the particle  $V(x, t)$  is the potential,  $T(x, t)$  is the temperature of the environment,  $\gamma$  is the viscous drag coefficient of the particle and  $k_B$  is the Boltzmann constant. Intuitively, the first term of the equation represents the (can we call this force conservative? this is true for time independent potentials, but we just wrote down a time dependent one ) force that the potential applies on the particle and the second term represents the diffusion of the particle due to thermal noise.

## 1.2 Brownian motors

Brownian motors are devices that can use stored chemical energy to create directed motion on a microscopic scale, they are ubiquitous in biology where they are used to perform important tasks in cells [13, 14] this is done by transforming energy from one degree of freedom to another. Recently, thanks to improvements in imaging techniques, researchers have been able to make highly detailed images of these motors and their working components [15]. As well as being able to crank a rotor in the in the fashion of a traditional motor, Brownian motors are also able to pump ions against a gradient and translocate molecules [2, 14, 16, 17]. Brownian motors have also been investigated in the laboratory, for example Ref [18] created a stochastic heat engine by placing a single colloidal particle in a time dependent optical trap. Likewise, Ref [19] placed a colloidal particle in an optical tweezer and drove the particle with explosive vaporization of the surrounding liquid, thus demonstrating a thermal mechanism for Brownian motors. Ref [20] placed DNA molecules in a time dependent potential to transport the molecules. Brownian ratchets capable of walking along a track have been implemented in the laboratory recently [21–23], in order to improve on these designs and to approach the efficiency present in nature, we will have to understand the physics of Brownian dynamics very clearly.

The name Brownian motors is not a misnomer, a Brownian motor can be modeled as a Brownian particle diffusing over its free energy landscape [2], in the case of Brownian motion it is natural to think of the particle moving in a spatial coordinate  $x$ , however in the case of Brownian motors the interpretation of the coordinate  $x$  is more abstract. In general  $x$  will be a degree of freedom for the system, examples include reaction coordinates for a chemical reactions, or in the case of a rotary motors, the angle of the motor itself.

## 1.3 Classes of Brownian motors

Here we will discuss different classes of Brownian motors and their relationship to the project. Different types of Brownian motors have been explored in the literature, including the Feynman ratchet [24], the Landauer blowtorch [25], thermal ratchets [19], time dependent potentials [18, 20] and tilted periodic potentials [14, 16].

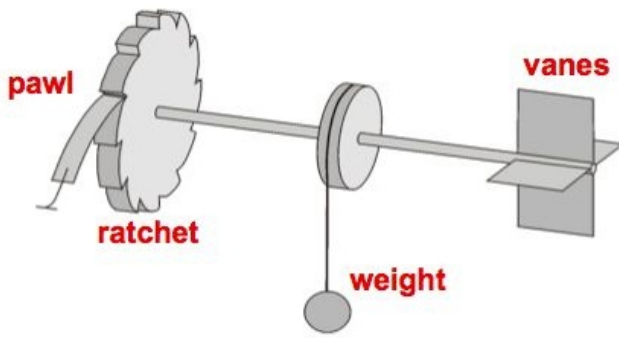


**Figure 1.3: The Feynmann ratchet and pawl [24].** The ratchet is located in a bath at temperature  $T_1$  and the vanes are in a bath at temperature  $T_2$ . (Figure taken from <http://pof.tnw.utwente.nl/research/granular/ratchet>)

### 1.3.1 Feynman ratchet and pawl

The Feynman ratchet was initially discussed in the Feynman lectures [24], it is an intuitive picture of how a motor may work at the microscopic scale and was at first thought to be able to achieve Carnot efficiency, however closer analysis showed that this was not possible [26]. The system works as follows, we have two boxes that are thermally insulated from one another that are connected by an axle that can rotate, these two boxes are at temperature  $T_1$  and  $T_2$  where in general  $T_1 \neq T_2$ . In one box there is a ratchet and pawl connected to the axle that makes it easy for the axle to turn one way (say clockwise), but hard to turn the other way (anti-clockwise). In the other box the axle is connected to vanes that are being buffeted by a gas. The motion of the vanes are random since they are dictated by Brownian motion, so the purpose of the ratchet and pawl is to rectify the Brownian motion of these vanes. One may think that this could be used to extract energy from the environment (for example by using the axle to lift a weight), this is true but one may not attain Carnot efficiency. The problem is that the ratchet and pawl themselves will also be subject to random motion so sometimes the pawl will be lifted allowing the axle to turn anti-clockwise.

In the case where  $T_1 = T_2$ , the pawl will be lifted just as frequently as the vanes are turned and the system will make no nett progress, this occurs despite the asymmetry of the ratchet. In the case where  $T_2 > T_1$ , the vanes will be moving quite frequently and we will find that work can be extracted from the system. On the other hand, when  $T_2 < T_1$  the vanes will be turning infrequently but the pawl will spend most of its time in the up position, allowing the axle to turn either direction, thus causing the ratchet to have no nett motion. Feynmann then reasoned that when  $T_2 > T_1$ , the system could achieve Carnot efficiency in the quasi-static limit where the nett motion goes to zero, this is in close analogy to a macroscopic heat engine, however the reasoning turned out to be flawed. The flaw in Feynmann's reasoning was that he did not consider the intrinsic irreversibility of the system, one must note that although the two boxes may be thermally insulated, they will still exchange heat through the axle itself. In order for Carnot's efficiency to be realized, the process must be reversible, so Feynmann's ratchet cannot attain Carnot efficiency.

## Landauer's blowtorch

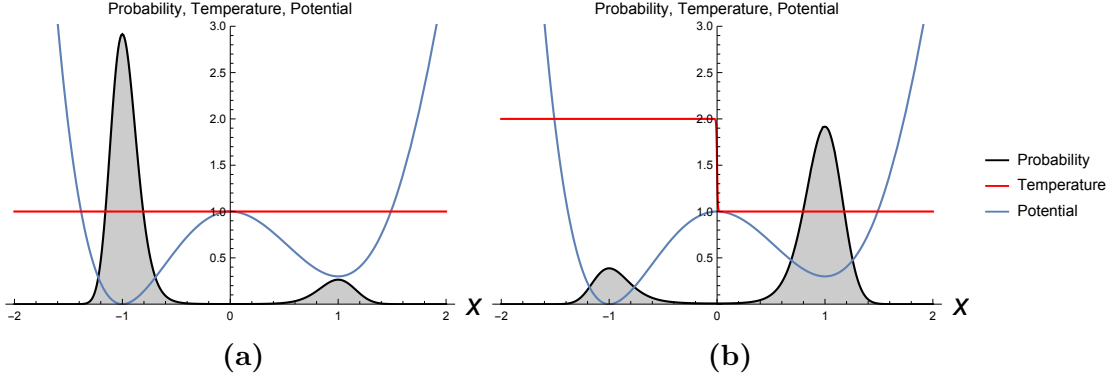


**Figure 1.4: Landauer's blowtorch in a bi-stable potential.** (a) we see that if the particles are left for a long enough time, then they will reach an equilibrium where the population in the upper well is less than that in the lower well. In (b) we see that if the temperature in the upper well is lower than that of the lower well, then the equilibrium concentrations are drastically altered.

To model the Feynman ratchet and measure it's efficiency, we will need two degrees of freedom [27], this is beyond the scope of this project because we will only simulate systems with one degree of freedom.

### 1.3.2 Landauer's blowtorch

The Landauer blowtorch scheme involves a temperature that varies in space [25]. The principle is shown schematically in Figure 1.4, in this figure the temperature is held fixed by an external heat source and can be made to vary along the potential. The steady state probability distribution was calculated using techniques that are described in § 3.1, in reference to this phenomena Landauer says that [25] “The relative occupation of competing states of local stability is not determined solely by the characteristics of the locally favored states, but depends on the noise along the whole path connecting the competing states.” The reason that particles move against the potential gradient is that where the potential is heated, the particles become more agitated, therefore we should expect that the probability of finding a particle in a hot region is small. A common analogy due to G. E. Hinton is pebbles on a driveway, if one places pebbles on a driveway in a uniform fashion, then after some time one will find that the pebbles will pile up on the side of the driveway where there is no traffic. This occurs despite the fact that the car exerts no nett sideways force on the pebbles, the explanation of this phenomena is that the car is agitating the pebbles in the center effectively at random, but once the pebbles leave the center they experience no agitation (zero temperature), so they will stay in place. This has caused some authors to describe the temperature as an effective potential [12, 28], in particular [29] report a so called reverse Landauer blowtorch effect. In their paper, the authors report that if one begins with particles in the upper well of a bi-stable potential, then as the particles move to the lower well, they will reduce the temperature of the upper well. In section § 4.1, we will discuss the reverse Landauer

blowtorch in more detail. The Landauer blowtorch is an important system because it clearly demonstrates that temperature gradients in stochastic systems need to be accounted for.

### 1.3.3 Tilted periodic potentials

The tilted periodic potential (Figure 1.2) is of particular interest for this project because it can be used to model biological motors [14, 16]. In this model, the potential can be a very complicated function of space despite the fact that temperature is held fixed. One way to model Brownian motors of this class is to think of a reaction coordinate  $x$  that describes the conformation of a molecule in a chemical reaction. An example of this is the reaction  $\text{ATP} \rightleftharpoons \text{ADP} + \text{P}$ , where ATP is adenosine triphosphate, ADP is adenosine di-phosphate and P is a lone phosphate molecule. This reaction coordinate is then coupled to a mechanical coordinate  $y$  so that each time that a reaction takes place, the motor will move in some way. Since this is a chemical reaction, the free energy will be decreased as time moves forwards. So a system that has a potential that is periodic in  $x$  is not sufficient to describe this situation, we will need to “tilt” the potential by adding a forcing  $f$ . The value of  $f$  will depend on the  $\Delta G$  of the reaction (i.e. how far out of equilibrium the reaction is). It is shown in [14] that this can be modeled by the two dimensional Smoluchowski equation. In this project we will only be modeling the one dimensional Smoluchowski equation, so we will have to consider the case where  $x$  and  $y$  are tightly coupled. An example of tight coupling is the kinesin motor [16] that is used in cells to transport molecules. The kinesin motor is strongly bound to a track that it “walks” along, on each step the motor will hydrolyze an ATP molecule using the reaction shown above. This reaction liberates about  $12k_B T$  Joules of energy that the motor uses to move forward. Kinesin motors are able to take many steps forward while taking few steps backwards all while falling off their track very infrequently [30].

## 1.4 Student contributions

The work of this honors project is as follows:



# Chapter 2

## Setting up the system

The law that entropy always increases, holds, I think, the supreme position among the laws of Nature. If someone points out to you that your pet theory of the universe is in disagreement with Maxwell's equations — then so much the worse for Maxwell's equations. If it is found to be contradicted by observation — well, these experimentalists do bungle things sometimes. But if your theory is found to be against the second law of thermodynamics I can give you no hope; there is nothing for it but to collapse in deepest humiliation.

---

**Arthur Eddington**  
– The nature of the physical world (1928)

### 2.1 The Smoluchowski equation

As we will see, the diffusion of a Brownian particle is increased by increasing the temperature, while the derivative of the potential describes the external force on the particle. In some cases such as the Landauer blowtorch, the environment has a non uniform temperature held fixed by an external heat source. With this in mind, we interpret Figures 1.2 and 1.4 as follows: Brownian particles are subject to a given potential and are agitated by thermal noise, these agitations can give the particles the energy to move over barriers created by the potential. As one could imagine, these thermal interactions draw energy from the environment as noted in Figure 1.1, one may imagine that these interactions could cause temperature of the environment to change. Normally two simplifying assumptions are made at this point [2], (i) that the thermal fluctuations created by the motor are very small compared to the thermal energy of the surrounding environment which is assumed to be effectively infinite, (ii) that when these temperature fluctuations occur, they diffuse away so rapidly that they do not need to be accounted for. In this project, we will question the second assumption, the aims of this project are as follows:

- Determine a consistent physical description of Brownian motion involving self-induced temperature gradients, this description must be consistent with the laws of thermodynamics as well as capturing the intuition that we have developed so far.

- Explore how this model differs from previous models of Brownian motion
- Determine conditions under which the model becomes the same as previous models of Brownian motion

The majority of the effort expended in this thesis will be in understanding the nature of two coupled partial differential equations, these take on the form:

$$J(x, t) = -\gamma^{-1} \frac{\partial}{\partial x} \left( \frac{\partial V(x, t)}{\partial x} P(x, t) + k_B T(x, t) \frac{\partial P(x, t)}{\partial x} \right) \quad (2.1)$$

$$\frac{\partial P(x, t)}{\partial t} = -\frac{\partial J}{\partial x} \quad (2.2)$$

$$\frac{\partial T(x, t)}{\partial t} = -\kappa q(x, t) + D \frac{\partial^2 T(x, t)}{\partial x^2} \quad (2.3)$$

Where

- $P(x, t)$  is the probability density as a function of reaction coordinate  $x$  and time  $t$
- $J(x, t)$  is called the current
- $\gamma$  is the friction coefficient and has units  $m^2 s^{-1}$
- $V(x, t)$  is the potential for the motor
- $k_B$  is the Boltzmann constant, units  $JK^{-1}$
- $q(x, t) = \partial_x V(x, t) J(x, t)$  is the heat from the motor [27]
- $\kappa$  is dictates how much the motor effects the environment, in § 2.2 we will show that  $\kappa$  is one over the specific heat of the environment
- $D$  is the thermal diffusivity and has units  $m^2 s^{-1}$

Equation (2.2) is called the Smoluschowski equation which we noted earlier and equation 2.3 is the heat equation. These equations make our intuitive notions more precise, we see that the first term on the right hand side of the Smoluchowski equation (equation 2.2) is a drift term that is forced by our potential and that the second term contains a diffusion term that is scaled by our temperature. Likewise, equation (2.3) also appeals to our intuition of how the motor should effect its environment. The first term represents the heat flux being produced by the motor [27], while the second term represents the diffusion of temperature into the environment. This model includes a temperature that depends on  $x$  and  $t$ , which has been explored in the literature [31]. Some authors write the current as [citations]

$$J(x, t) = -\gamma^{-1} \frac{\partial}{\partial x} \left( \frac{\partial V(x, t)}{\partial x} P(x, t) + k_B \frac{\partial}{\partial x} (T(x, t) P(x, t)) \right) \quad (2.4)$$

the difference being that they put the temperature inside the inner derivative. We will return to this difference in § 2.2, where we will discuss the role that the current



has in the generation of entropy. Our model departs from previous work is that the temperature now depends on the evolution of the probability distribution as well. Coupled models of this type have been mentioned earlier by Streater [8–11], our work uses a similar model that was modified to suit our needs.

Intuitively, the first term in equation 2.3 will create temperature gradients and the second term will cause these temperature gradients to flatten out. If the first term dominates, then the temperature gradients will grow to a very large size. In this case, we have to concede that our model will no longer be relevant, in particular our model does not include phase changes, so at the very least we require that the temperature gradients do not cause the fluid that the particle is in to freeze. This can be done if one makes sure that the second term is not significantly smaller than the first. In section § 2.3 we will show that this puts a restriction on the characteristic energy of the potential. On the other hand, if the second term completely dominates, then any temperature gradients created by the Brownian particle will immediately diffuse away. In this regime, equation 2.3 will not have an effect on the evolution of the system and the model will be reduced to the Smoluchowski equation by itself. The regime that we are interested in is the regime where the first and second terms are both important, in this regime the Brownian particle will have an effect on the environment but this effect will not cause the system to behave in a way that causes our model to break down.

The other restriction that we must make to our model is that there is only a very small number of Brownian particles. This is because the temperature gradients can act as inter-particle interactions, to see this imagine that there are two particles moving about and creating temperature gradients. If one particle moves to a location where the other has created a temperature gradient, then it will be effected by the temperature gradient created by the other particle. Therefore, to model this, one would need to model the probability distributions of each particle separately and make sure that the interactions are accounted for. We stress this point because often people will use the Smoluchowski equation to describe the density of particles in a fluid. Interpreting  $P(x, t)$  in this way in the presence of self induced temperature gradients would neglect the inter-particle interactions and would not be an accurate description. Therefore, we will be careful to make sure that  $P(x, t)$  is used to model the probability distribution of a single colloidal particle, not many.

Temperature gradients that are self induced in Brownian dynamics have been known for some time, a particularly interesting example is the Soret-Dufour effect [45–48]. In this effect, the diffusion of the concentration of a species of molecules Reverse Landauer blowtorch We will explore this in § 4.1 where we discuss how our model adds to this

## 2.2 System thermodynamics

Equation 2.2 and equation 2.3 define equations of motion for our system, the system may be confined to a region  $\Omega$  embedded in a larger environment which interacts with our system through the boundary conditions. In this section, we will show that our equations of motion obey the first and second laws of thermodynamics.

The potential energy of the particle is  $U_P = \int_{\Omega} V(x)P(x)dx$  and the thermal

energy of the bath is  $c_p \int_{\Omega} T(x) dx$ , where  $c_p$  is the specific heat capacity of the environment, to see that this is the thermal energy consider the units of the quantity  $c_p T(x, t)$ . These are  $JK^{-1}K$ , so  $c_p T(x, t) dx$  is the heat content of an infinitesimal element  $dx$ . With this we have:

$$E(t) = \int_{\Omega} V(x) P(x, t) dx + c_p \int_{\Omega} T(x, t) dx \quad (2.5)$$

By using the Smoluchowski equation and the heat equation, we can differentiate with respect to time to get:

$$\frac{dE}{dt} = \int_{\Omega} V(x) \frac{\partial P}{\partial t} dx + c_p \int_{\Omega} \frac{\partial T}{\partial t} dx \quad (2.6)$$

$$= - \int_{\Omega} V(x) \frac{\partial J}{\partial x} + c_p \int_{\Omega} -\kappa J(x) \frac{\partial V}{\partial x} + D \frac{\partial^2 T}{\partial x^2} dx \quad (2.7)$$

$$= [V(x)J(x)]_{\partial\Omega} + \int_{\Omega} \frac{\partial V}{\partial x} J(x) dx - \kappa c_p \int_{\Omega} \frac{\partial V}{\partial x} J(x) dx + c_p D \left[ \frac{\partial T}{\partial x} \right]_{\partial\Omega} \quad (2.8)$$

Notice that if the middle two terms cancel, then the change in energy is equal to the flow of energy through the boundaries. Thus, the first law of thermodynamics requires that  $\kappa = \frac{1}{c_p}$ , physically we can understand this by looking at the first term of equation 2.3. When the heat capacity is small,  $\kappa$  becomes large and in this case, even a small amount of heat being produced by the Brownian particle will have a large effect on the evolution of the temperature. Conversely, if the heat capacity is large, then the heat produced by the Brownian particle will have a very small effect on the temperature. We therefore expect that equation 2.3 can be neglected in the case where the environment has a very large heat capacity compared to the heat being produced by the Brownian particle.

As for the entropy, we have [9]

$$S(t) = -k_B \int_{\Omega} P(x, t) \log(P(x, t)) dx + c_p \int_{\Omega} \log(T(x, t)) dx \quad (2.9)$$

The first term is the Gibbs entropy in the continuous case [32] and the second term is the entropy of an incompressible fluid [33]. Using the entropy of an incompressible fluid restricts the systems that can be modelled by our equations of motion, in particular we will not be able to treat Brownian particles suspended in a gas since a gas is compressible by definition. The courageous reader may want to use our model in the case of a compressible fluid, however in this case we can no longer guarantee this reader that entropy will increase for them. The goal of this project is not to create a system that models many different situations in nature, but rather to create a system that is self-consistent.

Differentiating the entropy with respect to time, we get

$$\frac{dS}{dt} = k_B \int_{\Omega} \frac{\partial J}{\partial x} + \frac{\partial J}{\partial x} \log P dx + c_p \int_{\Omega} \frac{1}{T} \left( -\kappa J \frac{\partial V}{\partial x} + c_p D \frac{\partial^2 T}{\partial x^2} \right) dx \quad (2.10)$$

$$= k_B \left( [J]_{\partial\Omega} + [J \log P]_{\partial\Omega} - \int_{\Omega} \frac{J}{P} \frac{\partial P}{\partial x} dx \right) - \int_{\Omega} \frac{J}{T} \frac{\partial V}{\partial x} + c_p D \int_{\Omega} \frac{1}{T} \frac{\partial^2 T}{\partial x^2} dx \quad (2.11)$$

We will denote the boundary terms with  $B(t) = k_B([J \log P]_{\partial\Omega} + [\frac{\partial J}{\partial x}]_{\partial\Omega})$ , now the change in entropy becomes:

$$\frac{dS}{dt} = - \int_{\Omega} k_B \frac{J}{P} \frac{\partial P}{\partial x} + \frac{J}{T} \frac{\partial V}{\partial x} dx + c_p D \int_{\Omega} \frac{1}{T} \frac{\partial^2 T}{\partial x^2} dx + B(t) \quad (2.12)$$

$$= \gamma \int_{\Omega} \frac{J^2}{TP} dx + c_p D \int_{\Omega} \frac{1}{T} \frac{\partial^2 T}{\partial x^2} dx + B(t) \quad (2.13)$$

where in the second equality we used the fact that  $J = -\gamma^{-1}(P \frac{\partial V}{\partial x} + k_B T \frac{\partial P}{\partial x})$ .

By noticing that

$$\frac{\partial}{\partial x} \left( \frac{1}{T} \frac{\partial T}{\partial x} \right) = -\frac{1}{T^2} \left( \frac{\partial T}{\partial x} \right)^2 + \frac{1}{T} \frac{\partial^2 T}{\partial x^2} \quad (2.14)$$

we can rewrite the second term of equation 2.13 as:

$$c_p D \int_{\Omega} \frac{1}{T} \frac{\partial^2 T}{\partial x^2} dx = c_p D \int_{\Omega} \frac{\partial}{\partial x} \left( \frac{1}{T} \frac{\partial T}{\partial x} \right) + \frac{1}{T^2} \left( \frac{\partial T}{\partial x} \right)^2 dx \quad (2.15)$$

$$= c_p D \int_{\Omega} \frac{1}{T^2} \left( \frac{\partial T}{\partial x} \right)^2 dx + c_p D \left[ \frac{1}{T} \frac{\partial T}{\partial x} \right]_{\partial\Omega} \quad (2.16)$$

If we define

$$\dot{S}_{gen} \equiv \int_{\Omega} \gamma \frac{J^2}{TP} + c_p D \frac{1}{T^2} \left( \frac{\partial T}{\partial x} \right)^2 dx \quad (2.17)$$

and

$$B(t) \equiv k_B \left( [J \log P]_{\partial\Omega} + \left[ \frac{\partial J}{\partial x} \right]_{\partial\Omega} \right) + c_p D \left[ \frac{1}{T} \frac{\partial T}{\partial x} \right]_{\partial\Omega} \quad (2.18)$$

Then we notice that the change in entropy is equal to a positive number  $\dot{S}_{gen}$  plus the entropy flowing through the boundaries, this is precisely the second law of thermodynamics. Furthermore, the generated entropy can be split into two terms, the first term is to be interpreted as the entropy generated by the Brownian particle; since the motion of the particle is random, as the Brownian particle diffuses we will become less certain of its position. The second term is the entropy generated by the diffusion of temperature gradients; if one studies the solutions to the heat equation, then one will find that any spikes in the temperature will flatten out and eventually the temperature will be uniform. This flattening out of the temperature is naturally associated with an increase in entropy.

As mentioned earlier, some authors write the current as  $J = -\gamma^{-1}(P \frac{\partial V}{\partial x} + k_B \frac{\partial(TP)}{\partial x})$  [12, 31], however if we use this definition of  $J$ , then  $\dot{S}_{gen}$  is not necessarily positive, our version of the current is supported by Streater [8–11] and will reduce to the other version in the case of constant temperature.

## 2.3 Making the equations dimensionless

Upon viewing equations 2.2 and 2.3, we see that there is a large number of constants that are set by the properties of the Brownian particle that we are modeling.

We would like to reduce the number of variables for two reasons (i) by reducing the number of variables we will hopefully gain a more concise physical description of the system (ii) having a small number of free variables is very convenient for creating a program to approximate the equations numerically, dimensionless equations tend to be less prone to numerical error because they avoid cases where small numbers are compared to large ones in a floating point system. Here we will non-dimensionalize the equations, to do this, introduce  $\bar{x} = \frac{x}{L}$ , then the Smoluchowski equation becomes

$$\frac{\partial P}{\partial t} = \gamma^{-1} \frac{1}{L^2} \frac{\partial}{\partial \bar{x}} \left( P \frac{\partial V}{\partial \bar{x}} + k_B T \frac{\partial P}{\partial \bar{x}} \right) \quad (2.19)$$

Now let  $E_0$  be the characteristic energy of the system, for a chemical reaction,  $E_0$  will be the  $\Delta G$  of the reaction and for a periodic potential,  $E_0$  will be the energy difference along one period. Now we introduce the dimensionless potential and the dimensionless temperature as  $\hat{V}(x) = \frac{V(x)}{E_0}$  and  $\hat{T}(x) = \frac{k_B T(x)}{E_0}$  respectively. Now the Smoluchowski equation becomes

$$\frac{\partial P}{\partial t} = \frac{E_0}{\gamma L^2} \frac{\partial}{\partial \bar{x}} \left( P \frac{\partial \hat{V}}{\partial \bar{x}} + \hat{T} \frac{\partial P}{\partial \bar{x}} \right) \quad (2.20)$$

Let  $\tau = \frac{E_0}{\gamma L^2}$  and  $\hat{P} = LP$ , with this we have:

$$\frac{\partial \hat{P}}{\partial \tau} = \frac{\partial}{\partial \bar{x}} \left( \hat{P} \frac{\partial \hat{V}}{\partial \bar{x}} + \hat{T} \frac{\partial \hat{P}}{\partial \bar{x}} \right) \quad (2.21)$$

Now we define  $\hat{J} = \frac{\gamma L^2}{E_0} J$ , applying these definitions to the equation for the temperature evolution, we find that:

$$\frac{E_0^2}{\gamma k_B L^2} \frac{\partial \hat{T}}{\partial \tau} = -\kappa \frac{E_0}{\gamma L^2} \hat{J}(\bar{x}) \frac{E_0}{L} \frac{\partial \hat{V}}{\partial \bar{x}} + \frac{D E_0}{k_B L^2} \frac{\partial^2 \hat{T}}{\partial \bar{x}^2} \quad (2.22)$$

Now let  $\alpha = \frac{\kappa k_B}{L}$  and  $\beta = \frac{D \gamma}{E_0}$ , then we have

$$\frac{\partial \hat{T}}{\partial \tau} = -\alpha \hat{J}(\bar{x}) \frac{\partial \hat{V}}{\partial \bar{x}} + \beta \frac{\partial^2 \hat{T}}{\partial \bar{x}^2} \quad (2.23)$$

As for the energy of the system, the dimensioned version is:

$$E(t) = \int P(x) V(x) dx + \frac{1}{\kappa} \int T(x) dx \quad (2.24)$$

Let  $\hat{E}(t) = \frac{E(t)}{E_0}$ , we have:

$$\hat{E}(t) = \int \hat{P} \hat{V} d\bar{x} + \frac{L}{k_B \kappa} \int \hat{T} d\bar{x} \quad (2.25)$$

$$= \int \hat{P} \hat{V} d\bar{x} + \frac{1}{\alpha} \int \hat{T} d\bar{x} \quad (2.26)$$

So our system depends on the parameters  $\alpha$  and  $\beta$  as well as the shape of the potential. Physically,  $\alpha$  represents how much the particle interacts with the environment thermally and  $\beta$  represents how quickly the temperature diffuses.  $\alpha$  has units

$m^{-1}$  and  $\beta$  has units  $m^2kg^{-1}$ . As the length scale of the system increases,  $\alpha$  will decrease, therefore the temperature gradients are negligible for large systems. We interpret this as meaning that the temperature gradients are much smaller than the system and can diffuse away quickly. As the characteristic energy of the system increases,  $\beta$  will decrease meaning that the diffusion of temperature will be negligible. We interpret this as meaning that for high energy systems, temperature gradients are created much faster than they can be diffused away.



# Chapter 3

## Solving the system

People either write code that works, or they don't.

---

Colin Fox – 2016

Now that we have determined that our system is physical and we have made insights into the qualitative nature of our system, we must build techniques for solving the system so that we can gain quantitative insights. We will begin in § 3.1 by using analytical techniques to find stationary solutions to our equations of motion.

### 3.1 Steady state solution

In order to see how the equations of motion behave with time, we have to resort to numerical methods (see section 3.2). However we note that for a given potential there will be a stationary solution that we will refer to as the “steady state”, given periodic boundary conditions, we will derive an analytical form for this steady state.

In the steady state, we have:

$$\frac{\partial P(x, t)}{\partial t} = 0 = \frac{\partial J}{\partial x} \quad (3.1)$$

$$\frac{\partial T(x, t)}{\partial t} = 0 = -\kappa q(x, t) + \frac{\partial}{\partial x} \left( D \frac{\partial T(x, t)}{\partial x} \right) \quad (3.2)$$

Suppose that we have the following boundary conditions:

$$P(x = 0) = P(x = L) \quad (3.3)$$

$$J(x = 0) = J(x = L) \quad (3.4)$$

$$\left. \frac{\partial T}{\partial x} \right|_{x=0} = 0 = \left. \frac{\partial T}{\partial x} \right|_{x=L} \quad (3.5)$$

where  $L$  is the length scale of the domain. Physically, these conditions say that the nett current flowing out of the boundaries is zero and that no heat escapes from

the system, thus the energy of the system is conserved. Section 5.2 of [12] gives the steady state current as:

$$J_s = \left[ \frac{2k_B T(L)}{\psi(L)} - \frac{2k_B T(0)}{\psi(0)} \right] P_s(0) \left[ \int_0^L dx' / \psi(x') \right]^{-1} \quad (3.6)$$

with  $\psi(x) \equiv \exp[-\int_0^x dx' \frac{\partial_x V(x')}{2k_B T(x')}]$ . Meanwhile, the density is:

$$P_s(x) = P_s(0) \left[ \frac{\int_0^x \frac{dx'}{\psi(x')} \frac{T(L)}{\psi(L)} + \int_x^L \frac{dx'}{\psi(x')} \frac{T(0)}{\psi(0)}}{\frac{T(x)}{\psi(x)} \int_0^L \frac{dx'}{\psi(x')}} \right] \quad (3.7)$$

In this case,  $J_s$  is a constant and  $P_s(0)$  is also a constant. Assuming that we know these constants it is now possible to find the steady state temperature. We have:

$$\frac{\partial T}{\partial t} = 0 = -\kappa J_s \partial_x V + D \frac{\partial^2 T}{\partial x^2} \quad (3.8)$$

In one dimension, 3.8 can be written as an ordinary differential equation of the form

$$T''(x) = \frac{\kappa J_s}{D} V'(x) \quad (3.9)$$

We can solve this equation by integrating both sides twice to give:

$$T(x) = \frac{\kappa J_s}{D} \int_0^x V(x') dx' + \xi x + d \quad (3.10)$$

for unknown constants  $\xi$  and  $d$ . By applying the boundary condition 3.5, we find that

$$T'(0) = 0 = \frac{\kappa J_s}{D} V(0) + \xi \quad (3.11)$$

$$T'(L) = 0 = \frac{\kappa J_s}{D} V(L) + \xi \quad (3.12)$$

This implies that either  $V(0) = V(L)$  or  $J_s$  is a function of  $x$ , so in the tilted case, we find that the steady state current is a function of  $x$ . In the case of a titled periodic potential it is not sensible to think of a steady state solution because there will always be a flow of the probability distribution. This will be associated with a flow of energy through the boundaries meaning that energy is no longer conserved.

On the other hand, if we have  $V(0) = V(L)$ , then we can solve for  $\xi$  to give:

$$\xi = -\frac{\kappa J_s}{D} V(0) \quad (3.13)$$

Later, we will see that it is possible to have a steady state in higher dimensions where the flow of heat from the environment can dissipate the heat produced by the Brownian particle. By recalling that  $E = \int_0^L P(x') V(x') dx' + c_p \int_0^L T(x') dx'$  we are able to find an expression for  $d$ . First, we will integrate the temperature from 0 to  $L$

$$\int_0^L T(x') dx' = \frac{\kappa J_s}{D} \int_0^L dx' \int_0^{x'} V(x'') dx'' + \xi \frac{L^2}{2} + Ld \quad (3.14)$$



Therefore,

$$d = \frac{1}{L} \left( c_p E - c_p \int_0^L P(x') V(x') dx' - \frac{\kappa J_s}{D} \int_0^L dx' \int_0^{x'} V(x'') dx'' + \xi \frac{L^2}{2} \right) \quad (3.15)$$

It would seem that one should be able to calculate the steady state current and density directly from the equations shown above. However, we notice that the constants  $J_s$  and  $P_s(0)$  have to satisfy equations (3.6), (3.7) and (3.10) while also satisfying the normalization condition  $\int_0^L P(x) dx = 1$ . To do this we define an objective function given by

$$obj(J_s, P_s(0)) = \left( J_s - \left[ \frac{2k_B T(L)}{\psi(L)} - \frac{2k_B T(0)}{\psi(0)} \right] P_s(0) \left[ \int_0^L dx' / \psi(x') \right]^{-1} \right)^2 \quad (3.16)$$

And we minimize this objective function with respect to  $J_s$  and  $P_s(0)$  under the constraint  $\int_0^L P(x) dx = 1$ . Another way to do this is to guess a steady state density and temperature and use finite differencing to simulate forward in time until the transients die out. As well as this, one can write down the system as an ordinary differential equation in one dimension, this coupled set of ODEs can be solved numerically using Runge Kutta algorithms.

## 3.2 Finite differences

Our one dimensional equations can be solved on a discrete grid by using the finite differences method, the main idea behind this strategy is to approximate derivatives with equations of the form:

$$\frac{df}{dx} \approx \frac{f(x-h) - f(x+h)}{2h} \quad (3.17)$$

for some small  $h$ , likewise the second derivative of a function is approximated with

$$\frac{d^2 f}{dx^2} \approx \frac{f(x-h) - 2f(x) + f(x+h)}{h^2} \quad (3.18)$$

In our simulations, we will use the Crank Nicolson scheme [34, 35] to solve the equations. From now on, we will use the notation that  $F(j\Delta x, n\Delta t) = F_j^n$ , the key equation for the Crank Nicolson scheme is:

$$\frac{P_j^{n+1} - P_j^n}{\Delta t} = \frac{1}{2} (F_j^{n+1} + F_j^n) \quad (3.19)$$

where  $F$  represents the right hand side of the equation that we are doing finite differences on. This is an implicit set of equations that we will need to solve, in particular one may notice that  $F$  needs to be estimated at the future time in order for the equation to make sense. We will linearize the problem by assuming that the quantities of interest do not change by much in one time step.

By applying finite differences to the dimensionless Smoluchowski equation (eq 2.21), we find that:

$$F_j^i = \frac{P_{j+1}^i \partial V_{j+1}^i - P_{j-1}^i \partial V_{j-1}^i}{2\Delta x} + \frac{T_{j+1}^i - T_{j-1}^i}{2\Delta x} \frac{P_{j+1}^i - P_{j-1}^i}{2\Delta x} + T_j^i \frac{P_{j+1}^i - 2P_j^i + P_{j-1}^i}{\Delta x^2} \quad (3.20)$$

where we omitted the hats for notational convenience. We make the following definitions:

$$\begin{aligned} a_j^{n+1} &= \frac{-2T_j^{n+1}}{\Delta x^2} \\ b_j^{n+1} &= \frac{\partial_x V_{j+1}^{n+1}}{2\Delta x} + \frac{T_{j+1}^{n+1} - T_{j-1}^{n+1}}{4\Delta x^2} \\ c_j^{n+1} &= -\frac{\partial_x V_{j-1}^{n+1}}{2\Delta x} - \frac{T_{j+1}^{n+1} - T_{j-1}^{n+1}}{4\Delta x^2} \\ a_j^n &= \frac{-2T_j^n}{\Delta x^2} \\ b_j^n &= \frac{\partial_x V_{j+1}^n}{2\Delta x} + \frac{T_{j+1}^n - T_{j-1}^n}{4\Delta x^2} \\ c_j^n &= -\frac{\partial_x V_{j-1}^n}{2\Delta x} - \frac{T_{j+1}^n - T_{j-1}^n}{4\Delta x^2} \end{aligned} \quad (3.21)$$

With these definitions, the Crank Nicolson scheme can be written down as follows:

$$\begin{aligned} -\frac{\Delta t}{2} a_j^{n+1} P_{j-1}^{n+1} + \left(1 - \frac{\Delta t}{2} b_j^{n+1}\right) P_j^{n+1} - \frac{\Delta t}{2} c_j^{n+1} P_{j+1}^{n+1} \\ = a_j^n P_{j-1}^n + \left(1 + \frac{\Delta t}{2} b_j^n\right) P_j^n + \frac{\Delta t}{2} c_j^n P_{j+1}^n \end{aligned} \quad (3.22)$$

This equation can be written in matrix form by defining the following matrices:

$$A = \begin{bmatrix} a_0^{n+1} & b_1^{n+1} & 0 & 0 & 0 & \dots & 0 \\ c_0^{n+1} & a_1^{n+1} & b_2^{n+1} & 0 & 0 & \dots & 0 \\ 0 & c_1^{n+1} & a_2^{n+1} & b_3^{n+1} & 0 & \dots & 0 \\ \vdots & \vdots & \ddots & \ddots & \ddots & \vdots & \vdots \\ 0 & \dots & \dots & c_{J-2}^{n+1} & a_{J-1}^{n+1} & b_J^{n+1} \\ 0 & \dots & \dots & \dots & c_{J-1}^{n+1} & a_J^{n+1} \end{bmatrix}, \quad P^{n+1} = \begin{bmatrix} P_0^{n+1} \\ P_1^{n+1} \\ \vdots \\ P_{J-1}^{n+1} \\ P_J^{n+1} \end{bmatrix} \quad (3.23)$$

$$B = \begin{bmatrix} a_0^n & b_1^n & 0 & 0 & 0 & \dots & 0 \\ c_0^n & a_1^n & b_2^n & 0 & 0 & \dots & 0 \\ 0 & c_1^n & a_2^n & b_3^n & 0 & \dots & 0 \\ \vdots & \vdots & \ddots & \ddots & \ddots & \vdots & \vdots \\ 0 & \dots & c_{J-2}^n & a_{J-1}^n & b_J^n \\ 0 & \dots & & c_{J-1}^n & a_J^n \end{bmatrix}, \quad P^n = \begin{bmatrix} P_0^n \\ P_1^n \\ \vdots \\ P_{J-1}^n \\ P_J^n \end{bmatrix} \quad (3.24)$$

With these matrices, the equation now becomes,

$$\left( \mathbb{1} - \frac{\Delta t}{2} A \right) \cdot P^{n+1} = \left( \mathbb{1} + \frac{\Delta t}{2} B \right) \cdot P^n \quad (3.25)$$

we interpret this equation as saying that half of a backwards Euler step acting on  $P^{n+1}$  is equal to half of a forward Euler step acting on  $P^n$ . We write the equation to step  $P$  forward one time step as

$$P^{n+1} = \frac{\mathbb{1} + \frac{\Delta t}{2} B}{\mathbb{1} - \frac{\Delta t}{2} A} P^n \quad (3.26)$$

Each time that we step forward using this equation we will be out by a factor, this means that at each step we will need to renormalize using the equation  $\int P(x)dx = 1$ . If we do not apply this normalization, then the norm of our vector will change dramatically during a simulation. In order to estimate the integrals involved, we used the Simpson's rule of integration.

Likewise, we can apply the Crank Nicolson scheme to the heat equation, (eq 2.23), by looking at the right hand side of this equation, we find that

$$F_j^i = -\alpha \left( P_j^i (\partial_x V_j^i)^2 + \frac{T_{j+1}^i - T_{j-1}^i}{2\Delta x} \partial_x V_j^i \right) + \beta \frac{T_{j+1}^i - T_j^i + T_{j-1}^i}{\Delta x^2} \quad (3.27)$$

Just like the discretized Smoluchowski equation, these equations can be written in matrix form. The temperature is normalized by assuming that the energy remains fixed, this will be true as long as no heat or current flows through the boundaries, i.e.  $J(x = a) = 0 = J(x = b)$  and  $\frac{\partial T}{\partial x}|_a = 0 = \frac{\partial T}{\partial x}|_b$ . In this case, the energy is constant and is given by  $E = \int P(x)V(x)dx + c_p \int T(x)dx$ , so each time that we step the temperature forward, we have to calculate the potential and thermal energy and then scale the temperature so that the total energy remains fixed.

Fortunately the matrices that we are dealing with are very sparse, so the program used to solve these equations can save on memory by calling sparse matrix libraries.

### 3.2.1 Boundary conditions

So far we have discussed how to solve the equations inside the domain of interest  $\Omega$ , however our equations of motion will require that we prescribe boundary conditions that the system must satisfy. The boundary conditions that have been implemented for this project are as follows:

- Dirichlet: The value of the solution is specified at the boundaries
- Neumann: The value of the first derivative of the solution is specified at the boundaries
- Periodic: The value at the boundaries is not specified, but the left and right boundaries must take on the same value

Each type of boundary conditions comes along with its own physical interpretation, first we will deal with the boundary conditions imposed on the probability distribution.

If the potential goes to infinity at the boundaries, then the probability distribution must vanish at the boundaries before applying boundary conditions at all, therefore no boundary conditions need to be applied. There are some potentials that are periodic where the value of the potential is the same finite number at both sides, in this case it can be interesting to apply periodic boundary conditions to the probability distribution. Physically, this corresponds to a system where a particle passing through the left side will appear at the right side and vice-versa. One can picture this by imagining a particle constrained to a circular domain.

As for the temperature, both Neumann and Dirichlet boundary conditions are realized. In the case of Neumann boundary conditions, the derivative was set to zero at both boundaries. This is a very interesting case to imagine, because the derivative of the temperature physically represents the flow of heat in our system. Therefore the physical interpretation of a vanishing derivative at the boundary is that no heat is flowing through the boundaries, or in other words the system is enclosed in a perfectly insulating box. This system conserves energy, which is convenient when one goes to renormalize the calculated temperature by using the energy of the system.

The second type of boundary condition that can be imposed on the temperature is the Dirichlet type where the value of the temperature is specified at both boundaries. The physical interpretation of this requirement is that the domain is embedded in a much larger system that is at a fixed temperature. The tacit assumption made is that no matter what the system does, it is not able to affect the temperature of the environment. One must take care when using the energy to renormalize when considering Dirichlet boundary conditions, this is because the energy in the system is no longer conserved. To account for this, we calculate the heat flowing through the boundaries at each step and subtract this from the energy of the system before we renormalized the system.

Implementing these boundary conditions requires that we change our matrices  $A$  and  $B$ , specifically we will need to modify the top and bottom rows. The reason that we can do this is because a matrix represents a system of equations, the first and last rows of the matrices effect the first and last components of the vectors that we are doing finite differences on. For each boundary condition, we need to make sure that the equations represented by our first and last rows reflect our desired boundary conditions.

### Dirichlet boundary conditions

Imagine that we have a  $n \times n$  vector  $u$  that we want to step forward with finite differences while keeping the first and last components of  $u$  fixed. The equation for stepping  $u$  forward is given by:

$$u^{n+1} = \frac{\mathbb{1} + \frac{\Delta t}{2} B}{\mathbb{1} - \frac{\Delta t}{2} A} u^n \quad (3.28)$$

This equation will certainly affect the first and last components of  $u$ , in order to avoid this, we need to make sure that the first and last rows of  $(\mathbb{1} + \frac{\Delta t}{2} B)$  and  $(\mathbb{1} - \frac{\Delta t}{2} A)$  are the same as the first and last rows of the identity matrix.

### Neumann boundary conditions

The derivative at the boundaries can be made to be zero at the boundaries by making sure that the first and last rows of our matrices represent the equations  $u_J - u_{J-1} = 0$  and  $u_0 - u_1 = 0$  respectively. This can be done by replacing the first row with  $\{1, -1, 0, \dots, 0\}$  and the last row with  $\{0, 0, \dots, 0, -1, 1\}$ .

### Periodic boundary conditions

Periodic boundary conditions state that  $u_0 = u_J$ , if this is true at step  $i$ , then we can make sure that it is true at step  $i + 1$  by modifying our matrix appropriately. To be more precise if our finite differences matrix takes the form of equation 3.23, then in order to have periodic boundary conditions we would have to modify it to read:

$$A = \begin{bmatrix} a_0^{n+1} & b_1^{n+1} & 0 & 0 & 0 & \dots & c_0^{n+1} \\ c_0^{n+1} & a_1^{n+1} & b_2^{n+1} & 0 & 0 & \dots & 0 \\ 0 & c_1^{n+1} & a_2^{n+1} & b_3^{n+1} & 0 & \dots & 0 \\ \vdots & \vdots & \ddots & \ddots & \ddots & \vdots & \vdots \\ 0 & \dots & \dots & c_{J-2}^{n+1} & a_{J-1}^{n+1} & b_J^{n+1} \\ b_J^{n+1} & \dots & \dots & c_{J-1}^{n+1} & a_J^{n+1} & \dots \end{bmatrix} \quad (3.29)$$

This is equivalent to stretching out the matrix in a periodic fashion, we note that the matrix for periodic boundary conditions cannot be written in tridiagonal form. When the matrices involved are tridiagonal, we can inform the compiler of our program so that it can use highly optimized routines for solving the equations. However, in the case of periodic boundary conditions, we simply inform the compiler that the matrices are sparse, this means that we do not get the same speed for periodic boundary conditions as we do for other boundary conditions.

All of these boundary conditions were implemented in Julia [36], the user can decide which boundary condition that they want through a keyword argument and then the program will implement finite differences for that boundary type.

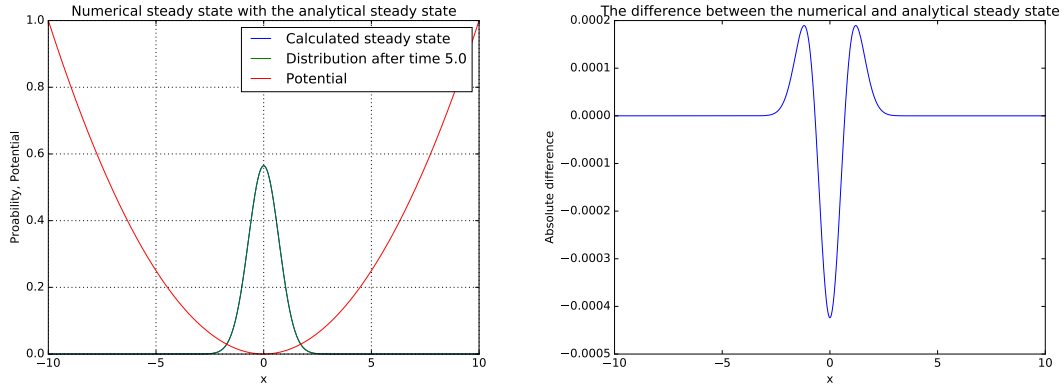


**Figure 3.1: Finite differences in the steady state.** The steady state for the system was calculated using equation 3.30, we start the system off in this state and then simulate the system forward 50,000 steps with  $\Delta t = 10^{-4}$  and  $\Delta x = 0.02$ . (a) shows the analytical steady state with the state after the simulation, (b) shows the absolute difference between these two vectors. Even after 50,000 steps the system has not deviated from the analytical steady state significantly.

### 3.3 Testing the numerics

The idea behind finite differences is that as the discretization size goes to zero, the numerical approximation should converge on the correct analytical solution. Here we will compare our numerics with some known analytical results as well as performing convergence tests.

#### 3.3.1 A comparison with analytical results

The Smoluchowski equation has a steady state probability density that takes on the form

$$P_{ss}(x) = N \exp \left( - \int_a^x \frac{V'(x')}{T(x')} dx' \right) \quad (3.30)$$

Figure 3.1 shows the a simulation where we began the system in the analytically calculated steady state, we then used finite differences to step forward 50,000 steps with  $\Delta t = 10^{-4}$ . After this simulation, we only found a minimal divergence from the steady state.

The heat equation can be solved using a Fourier series technique, in the case where there are no sources of heat, we have

$$\frac{\partial T}{\partial t} = \beta \frac{\partial^2 T}{\partial x^2} \quad (3.31)$$

the initial condition for the temperature will be denoted by,

$$T(x, 0) = f(x) \quad (3.32)$$

Lets say that the boundaries are at  $x = \pm\infty$  and that the derivative of the temperature is zeros at the boudaries. The solution to the heat equation is given

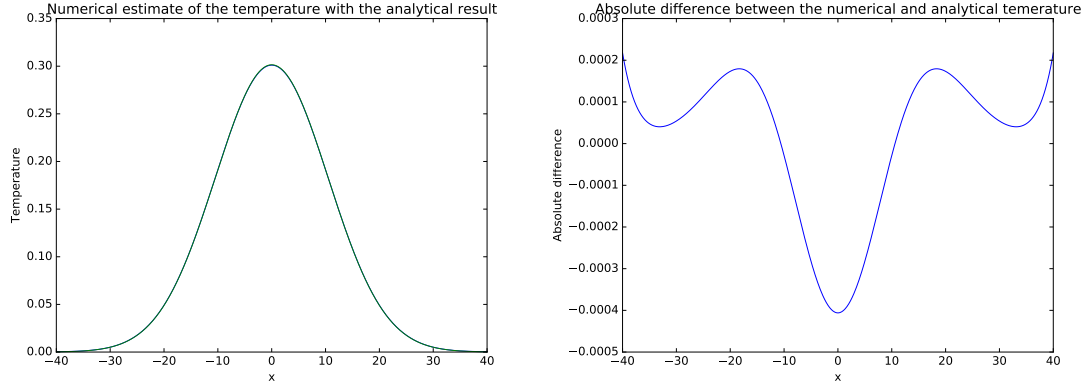


**Figure 3.2: Finite differences on the heat equation.** We simulate a situation where there are no sources for the heat equation and use equation 3.33 to obtain the analytical result we then compare this to the result of finite differences with  $\Delta t = 10^{-2}$  and  $\Delta x = 0.02$ .

by:

$$T(x, t) = \sum_{n=1}^{\infty} D_n \sin\left(\frac{n\pi x}{L}\right) \exp\left(\frac{-n^2 \pi^2 \beta t}{L^2}\right) \quad (3.33)$$

where

$$D_n = \frac{2}{L} \int_0^L f(x) \sin\left(\frac{n\pi x}{L}\right) dx \quad (3.34)$$

Say that we begin with a Gaussian function for the temperature, so that:

$$T(x, 0) = f(x) = \exp\left(-\frac{x^2}{4\beta}\right) \quad (3.35)$$

then as time goes on, the solution will become:

$$T(x, t) = \frac{1}{\sqrt{t+1}} \exp\left(-\frac{x^2}{4\beta(t+1)}\right) \quad (3.36)$$

We can compare these analytical results to the numerical ones obtained through finite differences, this is done in Figures 3.1 and 3.2. These figures show that even after many steps, the calculated solution has not deviated from the analytical one.

### 3.3.2 Convergence tests

If the finite differences methods that we have implemented are correct, then as the step size goes to zero, the numerical approximation will converge on the correct solution to the underlying equation being approximated. In the previous section we showed that finite differences approximated the solution very closely in some instances where the analytical result could be obtained. In general, we will not have an analytical solution to compare to but we would still like to be able to quantify the performance of our techniques.

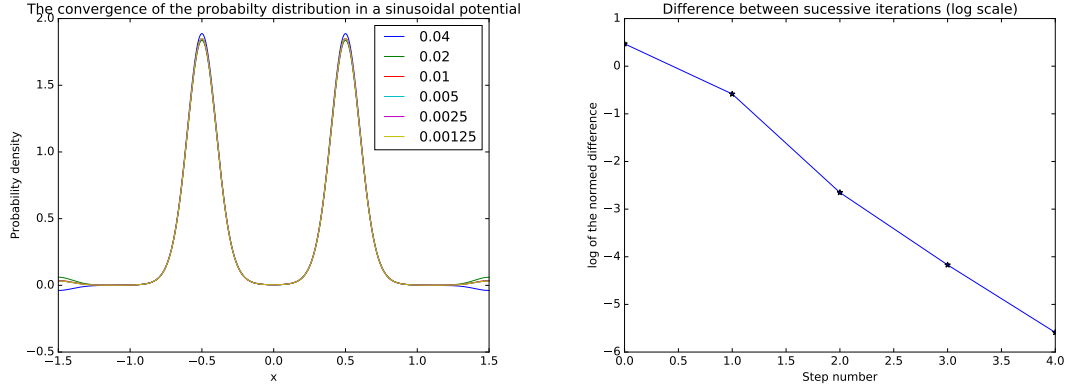


**Figure 3.3: The convergence of the probability distribution.** As  $\Delta t$  is decreased, the spatial discretization  $\Delta x$  is kept constant at 0.006. (a) the Smoluchowski equation is simulated forward for 1.0 seconds each line shows the result with a different value of the time step  $\Delta t$ . (b) the normed difference between each of the successive vectors is calculated and the result is plotted on a log scale, the slope of this graph is called the convergence rate.

Convergence tests involve decreasing the discretization size and checking whether the numerical solutions converge at all. In Figure 3.3, the Smoluchowski equation was simulated while keeping the temperature fixed, each time we halve  $\Delta t$  and measure the normed difference between the new result and the previous one.

Likewise, we can do convergence tests for the coupled system, for brevity we have only included the results for the evolution of the temperature. All of these plots show that the approximation converge exponentially to a particular solution, the convergence tests themselves do not prove that the numerical algorithms properly represent the equations `refeqn:dimensionlessSmoluchowski` and 2.23. However, combined with our analytical tests, they give us confidence that the numerics do agree with the true solution.

One can also perform convergence tests by increasing the number of points, from this one learns how sensitive the numerics are to the size of the spatial discretization  $\Delta x$ . This is shown in Figure 3.5, here we see that the temperature converges much more rapidly than the probability distribution does, however as  $\Delta x$  goes down, both converge exponentially.



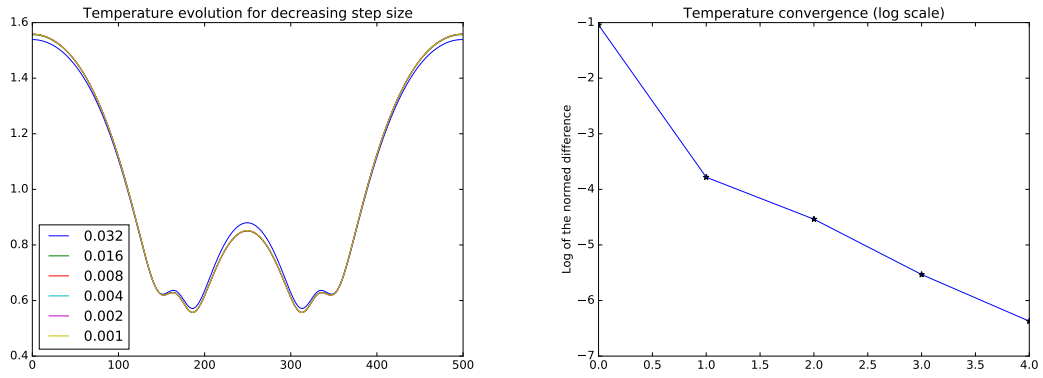


**Figure 3.4: The convergence of the temperature.** As  $\Delta t$  is decreased, the spatial discretization  $\Delta x$  is kept constant at 0.006. (a) the coupled equations are simulated forward for 1.0 seconds each line shows the temperature with a different value of the time step  $\Delta t$ . (b) the normed difference between each of the successive vectors is calculated and the result is plotted on a log scale.

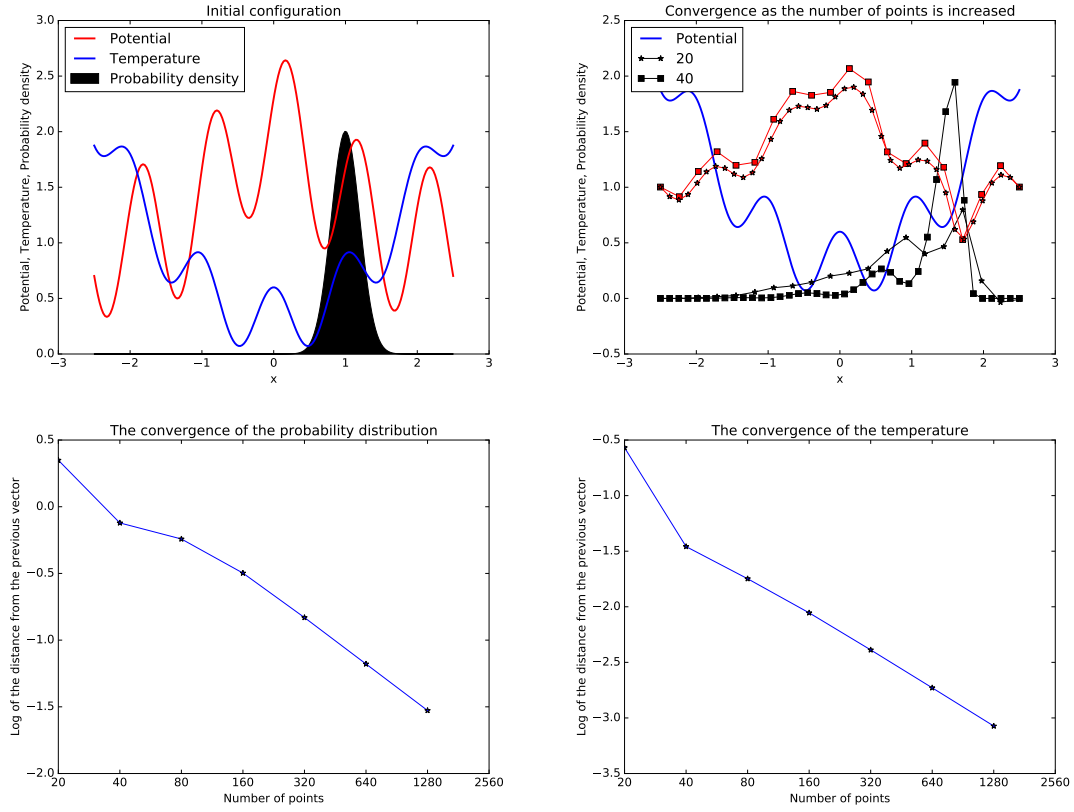


**Figure 3.5: Convergence tests for  $\Delta x$ .**  $\Delta t$  is held fixed at  $1 \times 10^{-5}$  and  $\alpha = 1 \times 10^{-2} m^{-1}$  and  $\beta = 0.1 m^2 kg^{-1}$ . (a) The initial configuration of the system, both the potential and the initial temperature are chosen to be complicated functions with large derivatives so that we can see how sensitive the numerics are to gradients. (b) The system after 40,000 steps forward in time, here we have not used the filling plot style to show the probability distribution so that one can see the difference between the different lines. (c) For each vector that was found through finite differences, we calculate its difference from the previous one, the  $x$  axis shows the length of each of the vectors. The  $y$  axis shows the log of these differences (d) Convergence of the temperature with an increasing number of points.

# Chapter 4

## Exploration

In that Empire, the Art of Cartography attained such Perfection that the map of a single Province occupied the entirety of a City, and the map of the Empire, the entirety of a Province. In time, those Unconscionable Maps no longer satisfied, and the Cartographers Guilds struck a Map of the Empire whose size was that of the Empire, and which coincided point for point with it. The following Generations, who were not so fond of the Study of Cartography as their Forebears had been, saw that that vast map was Useless, and not without some Pitilessness was it, that they delivered it up to the Inclemencies of Sun and Winters. In the Deserts of the West, still today, there are Tattered Ruins of that Map, inhabited by Animals and Beggars; in all the Land there is no other Relic of the Disciplines of Geography.

---

**Jorge Luis Borges and Adolfo Bioy Cesares**  
– “On Exactitude in Science”

Now that we have set up the framework for our system, we are able to discuss particular phenomena and their relation to nature. Here we will discuss some prototypical problems in stochastic systems and their behavior when considered in the light of equations 2.2 and 2.3. The point of this chapter is not to explain a particular experiment or the nature of a particular molecular motor in great detail. Nor is our aim to make a general model that may be easily adapted to any situation that the reader might fancy, but instead we aim to extract the physics that is at the essence of equations 2.2 and 2.3. We will find that our system differs from those previously explored, however the previous behavior may always be recovered by taking the limit of either high specific heat capacity or fast thermal diffusivity as discussed in § 2.3.

### 4.1 Bistable potentials

A bistable potential one that has two stable minima and an intermediate unstable maximum as depicted schematically in Figure 4.1, these potentials occur in a wide range of applications including digital logic [37, 38], protein folding [39] and chemical reactions [40]. The bistable potential well is one of the simplest ways to approach the Kramers’ rate and many other important properties of a stochastic system [37,

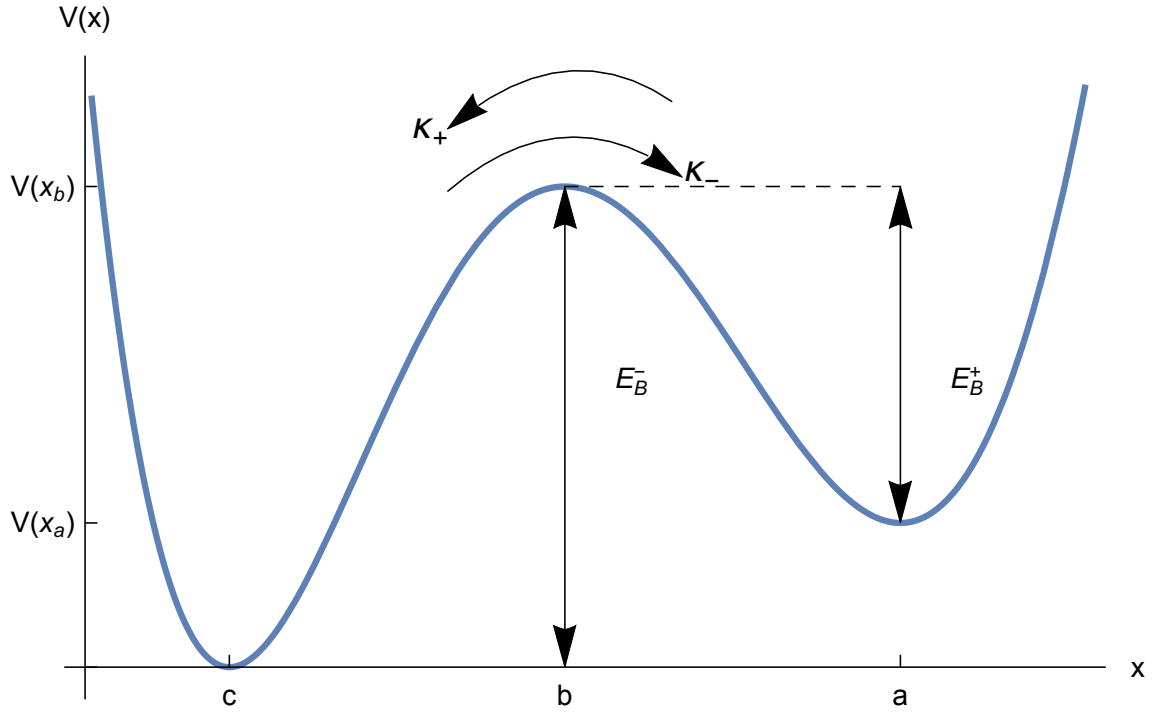


**Figure 4.1: Bistable potential.** In this plot we show the potential used to explore the Kramers rate and the reverse Landauer blowtorch, the potential has local minima at  $a$  and  $c$  and a maximum at  $b$ . If we begin with a probability distribution in the upper well, then the distribution will decay into the ground state of the upper well and then begin to decay into the lower well. The rate of flow from the upper well to the lower one will be denoted by  $\kappa_+$  and the rate of flow from the lower well into the upper one will be denoted by  $\kappa_-$ . In order for a Brownian particle to go from  $a$  to  $c$ , it will need to acquire thermal energy  $E_B^+$ , likewise to go from  $c$  to  $a$ , it will need energy  $E_B^-$ .

[41, 42]. In the context of Brownian motion, understanding the nature of bistable potentials can help one to build a master equation describing more complicated potentials comprised of multiple deep wells [41, 43].

#### 4.1.1 Kramer's rate

Consider the potential shown in Figure 4.1, if we begin in a state where we are certain that the particle is in the upper well, then as time passes, we should expect the probability distribution to move from point  $a$  over the barrier at  $b$  and into the well at point  $c$ . We will consider the regime where  $E_B^+ = V(x_b) - V(x_a) \gg k_B T$ , where  $T$  is constant, in this regime the rate at which the particles flow from  $a$  to  $c$  is given by the Eyring-Kramers' law [31, 44].

Say that the particle begins at  $a$ , we are interested in knowing how long it will take to reach a point  $x$ . This function is denoted by  $\tau(x)$  and is called the first passage time [12] the first passage time is associated with a density  $f(x, t)$ . In particular,  $f(x, t)$  denotes the probability that the particle has not passed the point  $x$  after a time  $t$ , given that the particle started at  $c$ . We would like to obtain the mean

first passage time  $\langle \tau(x) \rangle \equiv \int_0^\infty t f(x, t) dt$ , to do this we consider the dimensionless form of the Smoluchowski equation:

$$\frac{\partial P(x, t)}{\partial t} = \frac{\partial}{\partial x} (P(x, t) \partial_x V + T \partial_x P(x, t)) \quad (4.1)$$

we see that  $f(x, t)$  obeys the same equation of motion as  $P(x, t)$ . Integrating both sides yields:

$$\int_0^\infty dt \partial_t f(x, t) = \int_0^\infty dt \frac{\partial}{\partial x} (f(x, t) \partial_x V + T \partial_x f(x, t)) \quad (4.2)$$

using the fact that  $f(x, \infty) = 0$  and  $f(x, 0) = 1$ , we find that:

$$-1 = \frac{\partial}{\partial x} \left( -\langle \tau(x) \rangle \partial_x V + T \frac{\partial \langle \tau(x) \rangle}{\partial x} \right) \quad (4.3)$$

Since time dependence has been removed and we are only in one dimension, this is an ordinary differential equation for  $\langle \tau(x) \rangle$ . We notice that,

$$\frac{d}{dx} \left[ \exp \left( -\frac{V(x)}{T} \right) \frac{d}{dx} \langle \tau(x) \rangle \right] = \frac{1}{T} \exp \left( -\frac{V(x)}{T} \right) \left( -V'(x) \frac{d}{dx} \langle \tau(x) \rangle + \frac{d^2}{dx^2} \langle \tau(x) \rangle \right) \quad (4.4)$$

meaning that

$$\frac{d}{dx} \left[ \exp \left( -\frac{V(x)}{T} \right) \frac{d}{dx} \langle \tau(x) \rangle \right] = -\frac{1}{T} \exp \left( -\frac{V(x)}{T} \right) \quad (4.5)$$

Integrating from  $-\infty$  to  $x$  we have:

$$\exp \left( -\frac{V(x)}{T} \right) \frac{d}{dx} \langle \tau(x) \rangle = -\frac{1}{T} \int_{-\infty}^x dz \exp \left( -\frac{V(z)}{T} \right) \quad (4.6)$$

Finally, integrating from  $a$  to  $x$  and using the fact that  $\langle \tau(a) \rangle = 0$ , we get:

$$\langle \tau(x) \rangle = -\frac{1}{T} \int_a^x dy \exp \left( \frac{V(y)}{T} \right) \int_{-\infty}^y dz \exp \left( -\frac{V(z)}{T} \right) \quad (4.7)$$

If the particle starts at  $a$ , then the potential in the first integrand can be approximated by the second order Taylor expansion around  $b$  and the second integrand will be approximated by an expansion around  $a$ , more explicitly:

$$V(y) \approx V(b) + \frac{V''(b)}{2} (x - b)^2 \quad (4.8)$$

$$V(z) \approx V(a) + \frac{V''(a)}{2} (x - a)^2 \quad (4.9)$$

So for the mean first passage time of particles going from  $a$  to  $c$  we find,

$$\langle \tau_{a \rightarrow c} \rangle = \frac{2\pi}{\sqrt{-V''(b)V''(a)}} \exp \left( \frac{V(b) - V(a)}{T} \right) \quad (4.10)$$

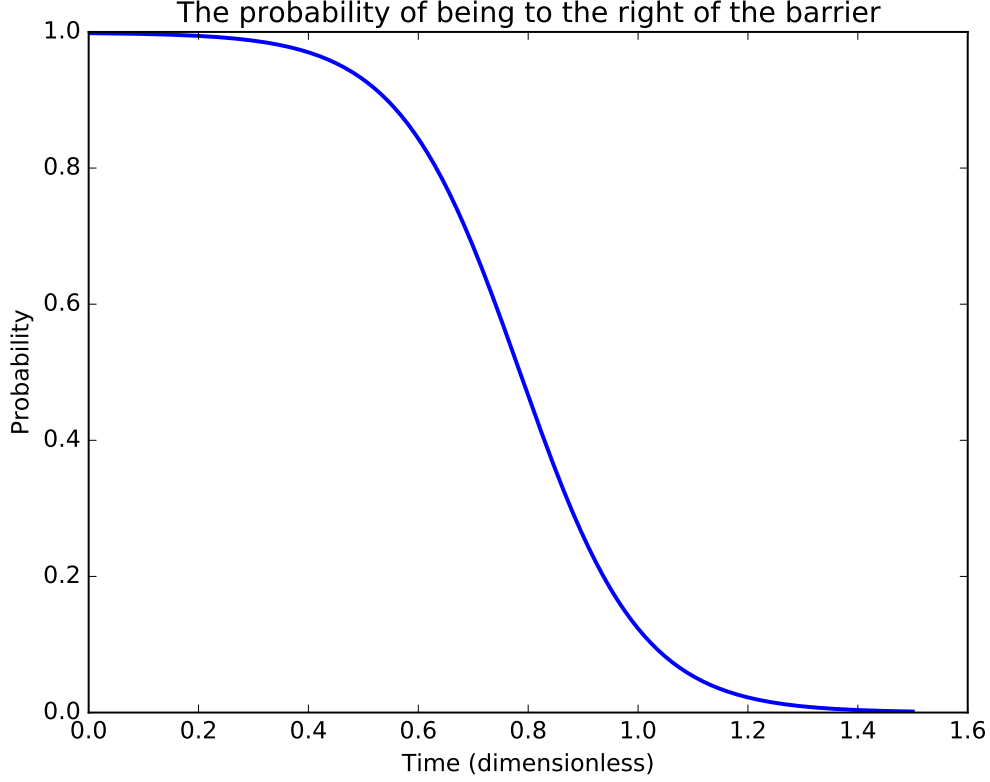


**Figure 4.2: The probability of being to the right of the barrier.** Here we see that the system decays into the ground state of the upper well and then begins to decay exponentially into the lower well. At the end of this, the probability of finding the particle on the upper well is almost zero. We can fit an exponential to this decay in order to estimate the Kramers' rate.

The Kramer's rate is given by one over the mean first passage time, we will denote the rate of particles moving from  $a$  to  $c$  as  $\kappa_+$ , which is given by:

$$\kappa_+ = \frac{\sqrt{|V''(b)V''(a)|}}{2\pi} e^{\frac{-E_B}{T}} \quad (4.11)$$

Likewise, there will be a current flowing from  $c$  to  $a$ , we will denote this by  $\kappa_-$ , once we have calculated both of these rates, the population in the upper well will be given by the differential equation

$$\frac{dP_+}{dt} = -\kappa_+ P_+(t) + \kappa_- P_-(t) \quad (4.12)$$

If we start with the population situated entirely in the upper well, then we get:

$$P_+(t) = \exp(-(\kappa_+ - \kappa_-)t). \quad (4.13)$$

We can also achieve this result numerically by starting the system off in the upper well and simulating forward while calculating the probability that the particle is in the upper well at each step. We then fit an exponential to this data and the fitted

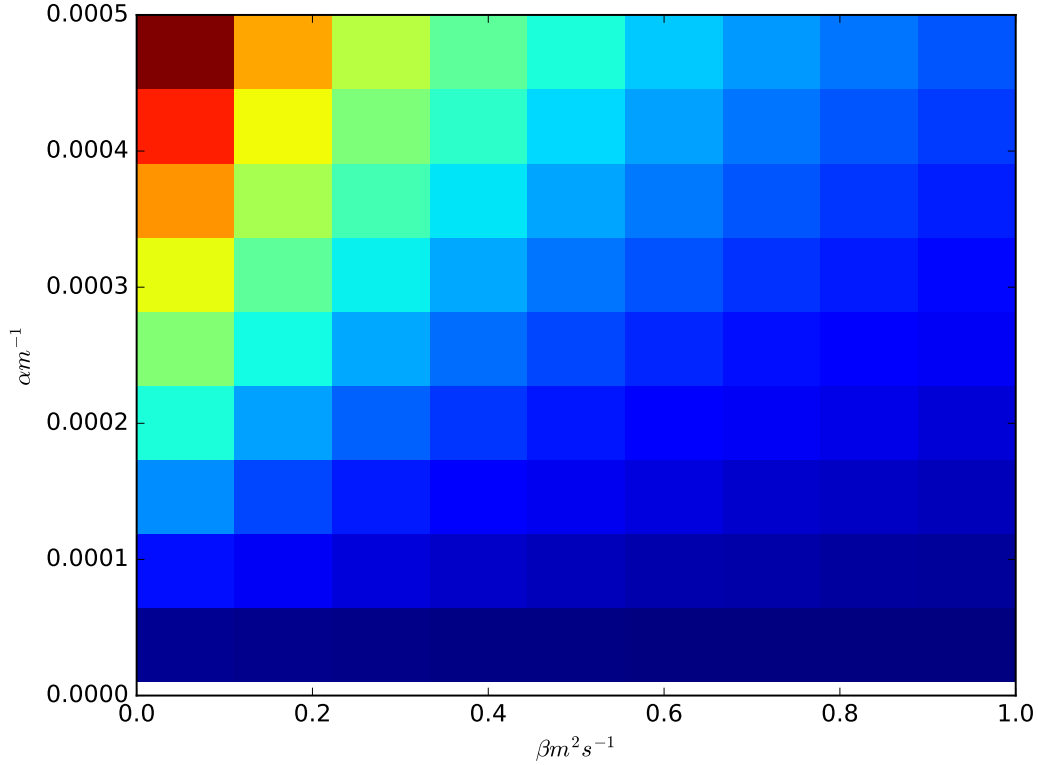


**Figure 4.3: Kramers' rate** Here we vary  $\alpha$  and  $\beta$  and perform the same measurements as in Figure 4.2, the results show that the Kramers' rate varies with  $\alpha$  and  $\beta$ .

rate will be our numerically estimated Kramers rate. To assist with measuring the Kramer's rate, we used Hermite interpolation to create a sixth order polynomial with the desired bistable shape. Specifically, we would allow  $V(x)$  to be a general 6th order polynomial and then we would specify the value of the polynomial at the locations  $a$ ,  $b$  and  $c$ , we would also enforce that the first derivative vanished at these locations. This would yield 6 equations which we would solve to give us the coefficients of  $V(x)$ , an example of such a polynomial is shown in Figure 4.1. Using these interpolating polynomials, we could keep the locations of the wells fixed while controlling the barrier height  $E_B^+$ . Once we had a potential, we would place the probability distribution in the upper well and then measure the probability that the particle is in the upper well with time and use this information to obtain the Kramer's rate, as shown in Figure 4.2.

This technique was used to calculate the Kramer's rate for multiple barrier height and potentials and it was found to be in excellent agreement with equation 4.10. The same technique can be used to obtain the Kramer's rate when the temperature is not held fixed. In this case, the Kramer's rate is sensitive to the boundary conditions imposed on the temperature and on the precise values of  $\alpha$  and  $\beta$  as shown in Figure 4.3.

We therefore conclude that the Kramer's rate is dependent on the heat capacity

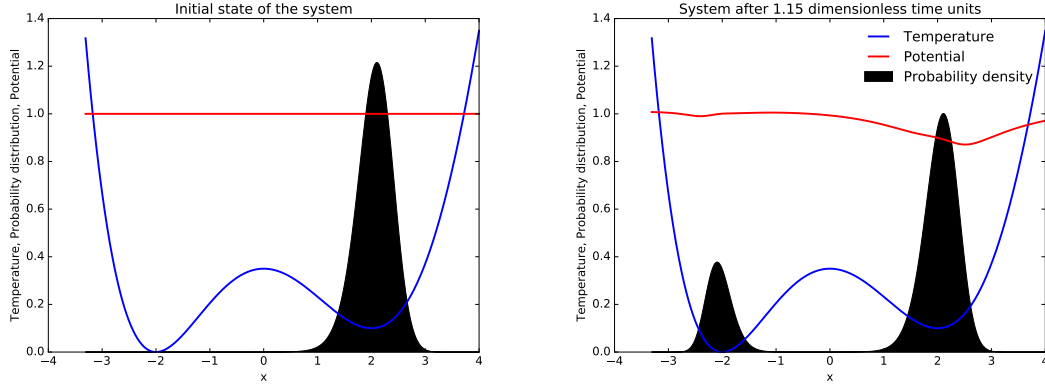


**Figure 4.4: Reverse Landauer blowtorch effect.** (a) The system starts off in the upper well of a bistable potential with a uniform temperature, we have  $\alpha = 1 \cdot 10^{-4} m^{-1}$  and  $\beta = 1 m^2 s^{-1}$ . (b) As the system decays into the lower well, the bath loses thermal energy in the form of heat, thus we see Brownian cooling as a consequence of the forcing of the potential. In these simulations, Dirichlet boundary conditions were imposed, meaning that the temperature at the ends was held fixed. This means that there was heat flowing through the boundaries, this heat was calculated at each time step and used to update the energy at each time step. This is necessary because the numerics use the energy to normalize the temperature as mentioned in § 3.2.

and thermal diffusivity of the system.

#### 4.1.2 The reverse Landauer blowtorch

As noted in subsection 1.3.2, the relative occupancy of wells depends on the spatial distribution of the temperature, meaning that the temperature can act as a pseudo-force. However, it has been noted that when the movement of the particle has an effect on the environment, the opposite can occur [29]. Concretely, the reverse Landauer blowtorch effect says that if there is a force applied to a Brownian particle, then the force will cause the particle to induce a temperature gradient in the environment. This is shown in Figure 4.4, in this figure, the temperature is held fixed at the boundaries, which we interpret physically as meaning that the domain is embedded in a much larger system that is held at a fixed temperature. Another example of a stochastic process that has an effect on the temperature of the environment is the Soret-Dufour effect [45–47], in the Soret effect or the Dufour effect, a non-equilibrium concentration of molecules is capable of producing a temperature gradient. Ref [48] showed that thermal gradients due to the Soret effect have to be taken into account to explain measurements performed on protein crystal growth. Despite the knowledge of these self induced temperature gradients, to our knowledge, Figure 4.4 is the first concrete observation of Brownian cooling as described by a self consistent theoretical model.



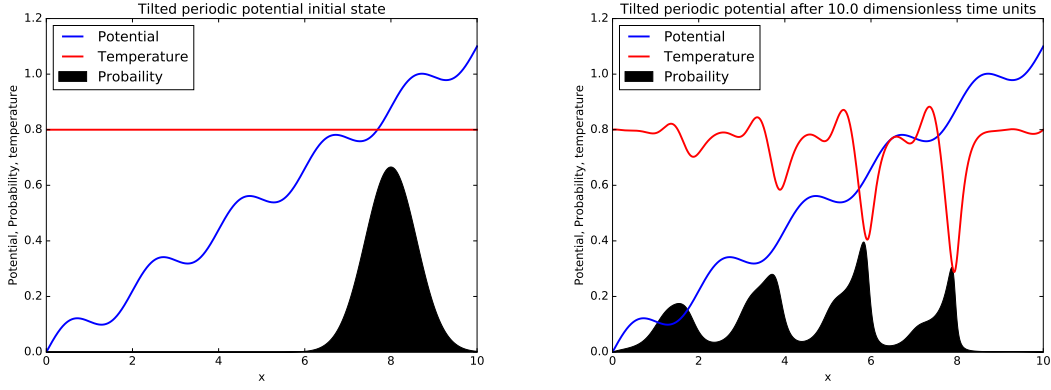


**Figure 4.5: Tilted periodic potential.** Imposing Dirichlet boundary conditions maintaining that the temperature is equal to 0.8 at the boundaries (temperature is dimensionless), we have  $\alpha = 1 \cdot 10^{-3} m^{-1}$  and  $\beta = 1 \cdot 10^{-2} m^2 s^{-1}$ . (a) The system begins with a uniform temperature with a Gaussian probability distribution located near the top of the potential. (b) after some time, the particle has moved down the potential, removing heat from the environment as it overcomes the periodic barriers provided by the potential. We notice that unlike Figure 1.2, the probability distribution does not decay into Gaussian distributions in the wells, instead the temperature gradients cause the probability distribution to take on a very complicated form.

## 4.2 Tilted periodic potentials

Tilted periodic potentials are very important in biology where they can be used to model molecular motors, in Ref [49, 50] the authors synthesize a tilted periodic potential by placing Brownian particles on a crystalline surface. The surface is then tilted at an angle  $\theta$  relative to the normal defined by gravity, in their theoretical analysis, the authors assume a constant temperature and are therefore able to describe a non-equilibrium steady state. Interestingly, in section 3.1, we showed that our system does not have such a well defined steady state for tilted periodic potentials.

Despite not being able to easily calculate the steady state for titled periodic potentials, we can still explore the dynamical case as shown in Figure 4.5. The tilted periodic potential combines the physics of both the Kramers' rate and the reverse Landauer blowtorch as described in § 4.1. One can imagine the potential in Figure 4.5 as being a multi-stable potential as opposed to the bistable potential shown in Figure 4.1. In fact, noticing that the titled periodic potential is a multi-stable potential led the authors of Ref [43] to describe a periodic potential with a master equation that involved the Kramers' rate of each of the adjacent wells. As well as the return of the Kramers' rate, Figure 4.5 is a very good demonstration of the reverse Landauer blowtorch effect. One can see from looking at the figure that the Brownian particle is absorbing heat from the environment as it moves down the potential. We therefore speculate that the reverse Landauer blowtorch effect could have an effect on biological molecular motors.



# Chapter 5

## Discussion

We have shown that self induced temperature gradients can play a crucial role in Brownian dynamics. Purely from a theoretical stand-point, such a model better explains the flow of energy and entropy through a system. In § 2.2 we explained how the temperature of the environment is a crucial player in the calculation of the entropy and energy of the system. The fact that our system has a well defined entropy is a strong advantage and allows one to talk about information in a rigorous way [37, 38].



# Chapter 6

## Outlook

This chapter will discuss possible future work and goals that are beyond the scope of this honors project, the main focus of this section is as follows:

- Generalization to 2d and 3d systems
- Inter-particle interactions
- Flow of heat via convection as well as an extension to compressible fluids and gases

### 6.1 Generalization to 2d and 3d systems

Many systems of interest are multi-dimensional and cannot be approximated by a one-dimensional system [1, 2, 14, 27, 43]. In particular, finding the efficiency of a molecular motor involves calculating the flow of energy from one degree of freedom to another [27]. Furthermore, generalizing our system to more dimensions gives more directions in which heat can flow, therefore allowing us to conserve energy in a more general sense **is this true? We can sort of do things without this by considering energy flows at the 1d boundaries.**

### 6.2 Inter-particle interactions

Inter-particle interactions play a very important role in Brownian dynamics [16, 17], an example of this is the myosin protein in cells which is used in the contraction of muscles [51]. Individually, myosin proteins are poor at carrying loads when compared to their kinesin counterparts [51], however their collective actions are very powerful due to the rich nature of their inter-motor interactions.

The set of equations that we have been using do not apply to more than one Brownian particle without some considerable changes. This is due to very complicated inter-particle interactions that can occur when considering thermal fluctuations of the kind that we are focusing on. To visualize this intuitively, imagine two particles diffusing in their reaction coordinates, both subject to the same potential. Particle one may induce local temperature gradients that will affect particle two if

particle two moves to where particle one created those temperature gradients. These interactions involve second order statistics that are beyond the scope of this project.

## 6.3 Fluid dynamics

The Brownian particles that we have been modelling have been suspended in a fluid. The dynamics of fluids present a formidable and exciting challenge to both physicists and mathematicians alike [citations], as well as this there has been effort in the literature to combine the Smoluchowski equation with the Navier-Stokes equation, thus linking the world of Brownian dynamics with fluid dynamics [52]. The two physical phenomena that we neglect which could be treated with techniques from fluid dynamics are compressible fluids and heat convection through fluid flow. Despite the fact that we neglected these phenomena, our system is still physical and is self consistent.

In section 2.2, in order to gain insight on the entropy we had to assume that we were dealing with an incompressible fluid. Without this assumption, we would not be able to guarantee that our equations of motion increase the entropy. Therefore, in order to obey the laws of thermodynamics in a compressible fluid, we would have to include extra terms in our equations of motion.

The second important phenomena that can be described by fluid dynamics is fluid flow. This phenomena is responsible for heat transport via convection, currently we only consider heat flow via diffusion, this means that we are tacitly assuming that the fluid in which our Brownian particle is suspended, is stationary. Including convection into our model would involve modifying the heat equation (equation 2.3) so that it reads

$$\frac{\partial T}{\partial t} + u(x)\frac{\partial T}{\partial x} = -\kappa J\partial_x V + D\frac{\partial^2 T}{\partial x^2} \quad (6.1)$$

Where  $u(x)$  represents the flow of the fluid, one can imagine that such a flow would have an effect on the system by transporting the temperature gradients with the flow of the fluid. The next step in including fluid dynamics into the system would be to introduce the Navier-Stokes equations into our system, thus yielding three coupled equations to solve.

# Bibliography

- [1] David Keller and Carlos Bustamante. The Mechanochemistry of Molecular Motors. *Biophysical Journal*, 2000.
- [2] Peter Reimann. Brownian Motors: noisy transport far from equilibrium. *Physics Reports*, 2001.
- [3] R Dean Astumian. Design principles for Brownian molecular machines: how to swim in molasses and walk in a hurricane. *Physical Chemistry Chemical Physics*, 9(37):5067–5083, 2007.
- [4] G. E. Uhlenbeck and L. S. Ornstein. On the theory of the brownian motion. *Phys. Rev.*, 36:823–841, Sep 1930.
- [5] Robert Brown. A Brief Account of Microscopical Investigations on the Particles Contained in the Pollen of Plants. *Privately circulated in 1828*, 1828.
- [6] A Einstein. On the movement of small particles suspended in stationary liquids required by the molecular-kinetic theory of heat. *Ann. Phys*, 17:549–560, 1905.
- [7] Jean Perrin. *Brownian movement and molecular reality*. Courier Corporation, 2013.
- [8] R. F. Streater. Non linear heat equations. *Reports on Mathematical Physics*, 1997.
- [9] R. F. Streater. A Gas of Brownian Particles in Statistical Dynamics. *Journal of Statistical Physics*, 1997.
- [10] R. F. Streater. The soiret and dufour effects in statistical dynamics. *Proceedings of the Royal Society of London A: Mathematical, Physical and Engineering Sciences*, 456(1993):205–221, 2000.
- [11] R. F. Streater. Dynamics of Brownian particles in a potential. *Journal of Mathematical Physics*, 38:4570–4575, September 1997.
- [12] Crispin Gardiner. *Stochastic methods*. Springer, 2009.
- [13] Rob Phillips and Stephen R. Quake. The Biological Frontier of Physics. *Physics Today*, May 2006.
- [14] Marcelo O. Magnasco. Molecular combustion motors. *Physical Review Letters*, 1994.

- [15] Anke Treuner-Lange Janet Iwasa Lotte Sogaard-Andersen Grant J. Jensen Yi-Wei Chang, Lee A. Rettberg. Architecture of the type IVa pilus machine. *Science*, 2016.
- [16] S Leibler and D A Huse. Porters versus rowers: a unified stochastic model of motor proteins. *The Journal of Cell Biology*, 121(6):1357–1368, 1993.
- [17] S Leibler and DA Huse. A physical model for motor proteins. *Comptes rendus de l’Academie des sciences. Serie III, Sciences de la vie*, 313(1):27–35, 1990.
- [18] Valentin Blickle and Clemens Bechinger. Realization of a micrometre-sized stochastic heat engine. *Nature Physics*, 2011.
- [19] Pedro A. Quinto-Su. A microscopic steam engine implemented in an optical tweezer. *Nature Communications*, 2014.
- [20] Steven A. Henck Michael W. Deem Gregory A. McDermott James M. Bustillo John W. Simpson Gregory T. Mulhern Joel S. Bader, Richard W. Hammond and Jonathan M. Rothberg. Dna transport by a micromachined Brownian ratchet device. *PNAS*, 1999.
- [21] Zhisong Wang. Bio-inspired track-walking molecular motors (perspective). *Biointerphases*, 5(3):FA63–FA68, 2010.
- [22] Max von Delius, Edzard M Geertsema, and David A Leigh. A synthetic small molecule that can walk down a track. *Nature chemistry*, 2(2):96–101, 2010.
- [23] Max von Delius, Edzard M Geertsema, David A Leigh, and Dan-Tam D Tang. Design, synthesis, and operation of small molecules that walk along tracks. *Journal of the American Chemical Society*, 132(45):16134–16145, 2010.
- [24] Richard Feynman. *Feynman lectures on physics*. California Institute of Technology, 1963.
- [25] Rolf Landauer. Motion out of noisy states. *Journal of Statistical Physics*, 53(1):233–248, 1988.
- [26] Juan M. R. Parrondo and Pep Español. Criticism of Feynman’s analysis of the ratchet as an engine. *American Journal of Physics*, 64(9):1125–1130, 1996.
- [27] C. Tumlin M. W. Jack. Intrinsic irreversibility limits the efficiency of multi-dimensional brownian motors. *Physical Review E*, 2016.
- [28] NG van Kampen. Explicit calculation of a model for diffusion in nonconstant temperature. *Journal of mathematical physics*, 29(5):1220–1224, 1988.
- [29] Moupriya Das, Debojyoti Das, Debashis Barik, and Deb Shankar Ray. Landauer’s blowtorch effect as a thermodynamic cross process: Brownian cooling. *Phys. Rev. E*, 92:052102, Nov 2015.
- [30] Schnapp BJ. Block SM, Goldstein LS. Bead movement by single kinesin molecules studied with optical tweezers. *Nature*, 1990.



- [31] Hendrik Anthony Kramers. Brownian motion in a field of force and the diffusion model of chemical reactions. *Physica*, 7(4):284–304, 1940.
- [32] Edward T Jaynes. Gibbs vs boltzmann entropies. *American Journal of Physics*, 33(5):391–398, 1965.
- [33] Yunus A Cengel and Michael A Boles. Thermodynamics: an engineering approach. *Sea*, 1000:8862, 1994.
- [34] J. Crank and P. Nicolson. A practical method for numerical evaluation of solutions of partial differential equations of the heat-conduction type. *Advances in Computational Mathematics*, 6(1):207–226, 1996.
- [35] William H Press. *Numerical recipes 3rd edition: The art of scientific computing*. Cambridge university press, 2007.
- [36] Jeff Bezanson, Alan Edelman, Stefan Karpinski, and Viral B. Shah. Julia: A Fresh Approach to Numerical Computing. *CoRR*, abs/1411.1607, 2014.
- [37] Christopher J Myers, Michele Celebrano, and Madhavi Krishnan. Information storage and retrieval in a single levitating colloidal particle. *Nature nanotechnology*, 10(10):886–891, 2015.
- [38] Rolf Landauer. Irreversibility and heat generation in the computing process. *IBM journal of research and development*, 5(3):183–191, 1961.
- [39] Joseph D Bryngelson and Peter G Wolynes. Intermediates and barrier crossing in a random energy model (with applications to protein folding). *The Journal of Physical Chemistry*, 93(19):6902–6915, 1989.
- [40] Bruce J Berne and Robert Pecora. *Dynamic light scattering: with applications to chemistry, biology, and physics*. Courier Corporation, 1976.
- [41] Victor Barcion. Eigenvalues of the one-dimensional Smoluchowski equation. *Journal of Statistical Physics*, 82(1):267–296, 1996.
- [42] I Santamaría-Holek, A Gadomski, and J M Rubí. Controlling protein crystal growth rate by means of temperature. *Journal of Physics: Condensed Matter*, 23(23):235101, 2011.
- [43] Katharine J Challis and Michael W Jack. Energy Transfer in a Molecular Motor in Kramers’ Regime. *Biophysical Journal*, 106(2):371a–372a, 2014.
- [44] Henry Eyring. The activated complex in chemical reactions. *The Journal of Chemical Physics*, 3(2):107–115, 1935.
- [45] Lars Onsager. Reciprocal relations in irreversible processes. i. *Phys. Rev.*, 37:405–426, Feb 1931.
- [46] W. Hort, S. J. Linz, and M. Lücke. Onset of convection in binary gas mixtures: Role of the dufour effect. *Phys. Rev. A*, 45:3737–3748, Mar 1992.

- [47] Roberto Piazza and Andrea Guarino. Soret effect in interacting micellar solutions. *Phys. Rev. Lett.*, 88:208302, May 2002.
- [48] I Santamaría-Holek, A Gadomski, and J M Rubí. Controlling protein crystal growth rate by means of temperature. *Journal of Physics: Condensed Matter*, 23(23):235101, 2011.
- [49] Xiao-guang Ma, Pik-Yin Lai, Bruce J Ackerson, and Penger Tong. Colloidal transport and diffusion over a tilted periodic potential: dynamics of individual particles. *Soft matter*, 11(6):1182–1196, 2015.
- [50] Xiao-guang Ma, Pik-Yin Lai, Bruce J Ackerson, and Penger Tong. Colloidal dynamics over a tilted periodic potential: Nonequilibrium steady-state distributions. *Physical Review E*, 91(4):042306, 2015.
- [51] Matthew J Tyska and David M Warshaw. The myosin power stroke. *Cell motility and the cytoskeleton*, 51(1):1–15, 2002.
- [52] Peter Constantin. Smoluchowski Navier-Stokes systems. *Contemporary Mathematics*, 429:85, 2007.

# Appendices



I am a fish.

---

**Philip Brydon – 2016**



# Appendix A

## Additional figures

There are a lot of interesting phenomena that occur when one explores the system that we explored in detail. In this appendix, we would like to share some of the exciting results that we found during the project, these results do not directly contribute to the narrative of the thesis which is why they were not included in the main body of the text. Despite not being a part of the main body, we feel that the reader would be at a loss without being made aware of these phenomena.

### Periodic boundary conditions

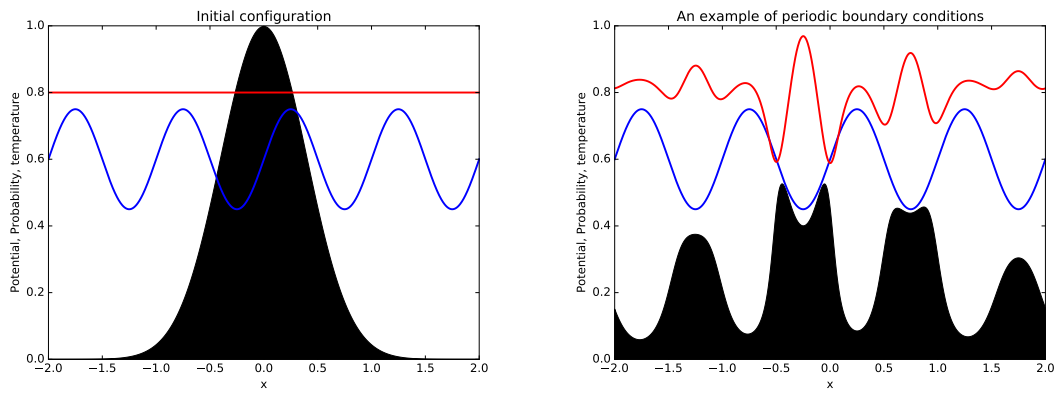


**Figure A.1:** An example of a periodic system visualized in one dimension. We have  $\alpha = 1 \cdot 10^{-2} m^{-1}$  and  $\beta = 1 \cdot 10^{-3} m^2 s^{-1}$